

In this paper, we describe an algorithm for approximating functions of the form $f(x) = \int_a^b x^\mu \sigma(\mu) d\mu$ over $[0, 1]$, where $\sigma(\mu)$ is some signed Radon measure, or, more generally, of the form $f(x) = \langle \sigma(\mu), x^\mu \rangle$, where $\sigma(\mu)$ is some distribution supported on $[a, b]$, with $0 < a < b < \infty$. One example from this class of functions is $x^c(\log x)^m = (-1)^m \langle \delta^{(m)}(\mu - c), x^\mu \rangle$, where $a \leq c \leq b$ and $m \geq 0$ is an integer. Given the desired accuracy ϵ and the values of a and b , our method determines a priori a collection of non-integer powers t_1, t_2, \dots, t_N , so that the functions are approximated by series of the form $f(x) \approx \sum_{j=1}^N c_j x^{t_j}$, and a set of collocation points x_1, x_2, \dots, x_N , such that the expansion coefficients can be found by collocating the function at these points. We prove that our method has a small uniform approximation error which is proportional to ϵ multiplied by some small constants, and that the number of singular powers and collocation points grows as $N = O(\log \frac{1}{\epsilon})$. We demonstrate the performance of our algorithm with several numerical experiments.

On the Approximation of Singular Functions by Series of Non-integer Powers

Mohan Zhao[†] \diamond and Kirill Serkh[‡] \diamond
University of Toronto NA Technical Report
v2, December 10, 2024

\diamond This author's work was supported in part by the NSERC Discovery Grants RGPIN-2020-06022 and DGECR-2020-00356.

[†] Dept. of Computer Science, University of Toronto, Toronto, ON M5S 2E4
Corresponding author. Email: mohan.zhao@mail.utoronto.ca

[‡] Dept. of Math. and Computer Science, University of Toronto, Toronto, ON M5S 2E4
Email: kserkh@math.toronto.edu

Keywords: *approximation theory, singular functions, singular value decompositions, corners, endpoint singularities, Laplace transforms, partial differential equations*

1 Introduction

The approximation of functions with singularities is a central topic in approximation theory. One motivating application is the efficient representation of solutions to partial differential equations (PDEs) on nonsmooth geometries or with discontinuous data, which are known to have branch-point singularities. Substantial progress has been made in this area, with perhaps the most common approach being rational approximation and its variants. Alternative approaches include the use of approximation methods for smooth functions on the real line, applied after a change of variables to ensure a rapid function decay and the translation of singularities to infinity, and schemes that make use of basis functions obtained through the discretization of certain integral operators. If the dominant characteristics of the functions to be approximated are known a priori, a class of methods called expert-driven approximation can also be used.

Rational approximation is a classical and well-established method for approximating functions with singularities. Rational functions $r(x) = p(x)/q(x)$ are said to be of type (n, m) if p and q are polynomials of degree at most n and m , respectively, and the order of $r(x)$ is defined as $\max(\deg(p), \deg(q))$. In 1964, Newman proved that there exists an n -th order rational approximation to the function $f(x) = |x|$ on $[-1, 1]$, converging uniformly at a rate of $O(\exp(-C\sqrt{n}))$ for some constant $C > 0$ [25]—compare this to the best polynomial approximation to $|x|$ on $[-1, 1]$, which can only achieve a convergence rate no better than $O(n^{-1})$. Furthermore, he observed that the same approximation also applies to the function $f(x) = \sqrt{x}$ and, more generally, to the functions $f(x) = x^\alpha$ on $[0, 1]$, where $\alpha > 0$. Notably, Newman’s approximation utilizes poles that are clustered exponentially and symmetrically around zero along the imaginary axis.

Numerous papers have been published on rational approximation methods for functions with singularities since Newman’s discovery (see, for example, [10], [32], [22], [7]). The best possible rational approximation is the so-called minimax approximation, which minimizes the maximum uniform approximation error between the function and its rational approximate. It was shown by Stahl in 1994 that error of the minimax approximation to $f(x) = x^\alpha$ on $[0, 1]$, where $\alpha > 0$, converges at the rate $O(\exp(-2\pi\sqrt{\alpha n}))$ [32]. This minimax approximation is, however, not easy to find, and is not necessarily unique in the complex plane [13]. In practice, by assuming that the singular functions being approximated fall into certain regularity classes, the poles of a rational approximation can often be determined a priori, similar to those employed in Newman’s method, in order to achieve a root-exponential convergence rate. One such method is Stenger’s approximation [33], which involves interpolating the functions at a set of preassigned points exponentially clustered near the endpoints of the interval, using a rational function of type $(2n + 2, 2n + 1)$ with poles that are likewise exponentially clustered at the endpoints.

While Stenger’s method uses explicit interpolation formulas for approximating functions falling into certain regularity classes, rational approximations can also be constructed numerically using other representations. By using Euclidean division and the method of undetermined coefficients, it is possible to show that any rational function $r(x)$ of type

$(n + m, n)$ with distinct poles can be written in the form

$$r(x) = \sum_{j=0}^m b_j x^j + \sum_{j=1}^n \frac{a_j}{x - z_j}. \quad (1)$$

In order to approximate functions with branch point singularities, lightning methods ([12], [11]) fix the poles in the representation (1) a priori to cluster exponentially along rays in the complex plane, terminating at the singular points of the function being approximated. The coefficients $\{a_j\}$ and $\{b_j\}$ are then determined by solving a least squares problem at oversampled points. It was proved in [12] that, for any sequence of n complex points exhibiting exponential clustering, with spacing scaling as $O(n^{-1/2})$ on a logarithmic scale, there exists a sequence of rational approximations $\{r_n\}$ of type $(n - 1, n)$ with poles at these points, which achieves a root-exponential rate of convergence $O(\exp(-C\sqrt{n}))$ for functions with branch point singularities.

Rather than fixing the poles of a rational function a priori, one can instead fix the interpolation or support points of a rational interpolant. As shown in [24], any rational function $r(x)$ of type (n, n) which does not have poles at the points $\{z_j\}$ can be written in the barycentric form

$$r(x) = \sum_{j=1}^{n+1} \frac{w_j f_j}{x - z_j} \bigg/ \sum_{j=1}^{n+1} \frac{w_j}{x - z_j}, \quad (2)$$

so that $r(z_j) = f_j$. The adaptive Antoulas-Anderson (AAA) algorithm [24] is a rational function approximation method based on this form, which increases the order n at each iteration, selecting the additional collocation point z_{n+1} in a greedy fashion. Like lightning methods, the weights are found by solving a least-squares problem. Unlike lightning methods, however, the locations of the singular points of the function being approximated do not have to be known in advance. The AAA method is also root-exponentially convergent, and achieves a convergence rate close to the minimax rate.

While all of the aforementioned methods can achieve root-exponential rates of convergence, Trefethen et al. [36] made a key observation that the constant C in the rates of convergence $O(\exp(-C\sqrt{n}))$ can be improved for most rational approximation methods by employing poles with so-called tapered exponential clustering around singularities, so that the poles $\{z_j\}$ cluster like $O(\sqrt{n} - \sqrt{j})$ on a logarithmic scale. It was shown in [16] that lightning approximations (1) with $m = O(\sqrt{n})$ and with poles $\{z_j\}$ with tapered exponential clustering attain the minimax rate for the functions $f(x) = x^\alpha$ on $[0, 1]$, where $\alpha > 0$.

Rational approximation can also be applied after a change of variables. An approach referred to as reciprocal-log approximation [23] uses approximations of the form $r(-\log x)$, where $r(s)$ is an n -th order rational function with poles determined a priori, either lying on a parabolic contour or confluent at the same point in the complex plane. Similarly to lightning methods, the coefficients are determined through a linear least-squares problem using collocation points that cluster exponentially around $z = 0$. This method converges at a rate of $O(\exp(-Cn))$ or $O(\exp(-Cn/\log n))$ for functions with branch-point singularities, depending on the form of the approximation and the function's behaviour in the complex plane.

An alternative approach is to use a combination of a change of variables and an approximation scheme that converges rapidly for smooth functions on the real line. By applying smooth transformations to functions with singularities at the endpoints of some finite intervals on the real line, they can be transformed into rapidly decaying functions, with the singularities mapped to the point at infinity. After this transformation, such functions can be approximated accurately using the Sinc approximation, by an n -term truncated Sinc expansion. Two primary approaches of this type have been developed: the SE-Sinc and DE-Sinc approximations (see, for example, [34], [26] and [21]). The SE-Sinc approximation combines the single-exponential transformation with the Sinc approximation, resulting in a convergence rate of $O(\exp(-C\sqrt{n}))$, while the DE-Sinc approximation combines the double-exponential transformation with the Sinc approximation, to further improve the convergence rate to $O(\exp(-Cn/\log n))$.

While the aforementioned methods require no special knowledge of the singularities being approximated, a class of methods known as expert-driven approximation can be used to leverage such information. For example, one can leverage knowledge of the leading terms in the asymptotic expansion of the singularity to achieve a smaller approximation error. This information is often available for the solutions of boundary value problems for PDEs on domain with corners—as revealed by Lehman ([19]) and Wasow ([38]), the solutions of the Dirichlet problem for linear second order elliptic PDEs in two dimensions have singular expansions of the form

$$u(r, \theta) \sim \sum_{k,m,l \geq 0} a_{k,m,l} r^{k+l/\alpha} (r^p \log r)^m \varphi_{k,m,l}(\theta), \quad (3)$$

where $\varphi_{k,m,l}$ are smooth functions, r is the radial distance from the corner, $\pi\alpha$ is the interior angle at the corner (so that $1/\alpha \geq 1/2$), and $p \geq 1$ is an integer. Many well-developed methods fall under the category of expert-driven approximation, such as the method of auxiliary mapping (see, for example, [20], [1]), in which an analytic change of variables is used to lessen the singular behaviour of the function, and enriched approximation methods (see, for example, [15]), in which singular basis functions are used to augment a conventional basis. Some examples of enriched approximation methods include extended/generalized finite element methods (see, for example, [27], [8], [9]), enriched spectral and pseudo-spectral methods (see, for example, [5], [12], [28]), and integral equation methods using singular basis functions (see, for example, [29] and [30]).

A much different class of approaches is based on the idea that the functions we are interested in approximating often belong to the range of certain integral operators. One such method proposed by Beylkin and Monzón [4] involves representing a function by a linear combination of exponential terms with complex-valued exponents and coefficients. This method is motivated by the observation that many functions admit representations by exponential integrals over contours in the complex plane, which can then be discretized by quadrature. Instead of starting with a contour integral, the existence of such representations is only assumed implicitly, and the exponents (which they also call nodes) are obtained by finding the roots of a c -eigenpolynomial corresponding to a Hankel matrix, constructed from uniform samples of the function over the interval, while the coefficients (or weights) are determined via a Vandermonde system. This method can be highly effective for representing functions, though we note that their method only minimizes the error at the sample points, and, for singular functions, they only try to control the error on a subinterval which excludes the singularities.

In this paper, we present a method for approximating functions with an endpoint singularity over $[0, 1] \subset \mathbb{R}$ or, more generally, a curve $\Gamma \subset \mathbb{C}$, where the functions have the form $f(x) = \int_a^b x^\mu \sigma(\mu) d\mu$, where $0 < a < b < \infty$, $x \in [0, 1]$ or $x \in \Gamma$, and $\sigma(\mu)$ is some signed Radon measure over $[a, b]$ or some distribution supported on $[a, b]$. Some examples of such functions are $x^c = \int_a^b x^\mu \delta(\mu - c) d\mu$ and $x^c (\log x)^m = (-1)^m \int_a^b x^\mu \delta^{(m)}(\mu - c) d\mu$, where $a \leq c \leq b$, $m \in \mathbb{Z}$ and $m \geq 0$. Our method represents these functions as expansions of the form $\hat{f}_N(x) = \sum_{j=1}^N \hat{c}_j x^{t_j}$, so that $\|f - \hat{f}_N\|_{L^\infty[0,1]} \approx \epsilon$, where the singular powers t_1, t_2, \dots, t_N are determined a priori based on the desired approximation accuracy ϵ and the values of a and b . The coefficients of the expansion are determined by numerically solving a Vandermonde-like collocation problem

$$\begin{pmatrix} x_1^{t_1} & x_1^{t_2} & \dots & x_1^{t_N} \\ x_2^{t_1} & x_2^{t_2} & \dots & x_2^{t_N} \\ \vdots & \vdots & \ddots & \vdots \\ x_N^{t_1} & x_N^{t_2} & \dots & x_N^{t_N} \end{pmatrix} \begin{pmatrix} c_1 \\ c_2 \\ \vdots \\ c_N \end{pmatrix} = \begin{pmatrix} f(x_1) \\ f(x_2) \\ \vdots \\ f(x_N) \end{pmatrix} \quad (4)$$

for $f(x)$ at the points x_1, x_2, \dots, x_N , where the collocation points are likewise determined a priori by ϵ , a and b . We both prove and show numerically that, in order to obtain a uniform approximation error of ϵ , the number of basis functions and collocation points grows as $N = O(\log \frac{1}{\epsilon})$.

Note that our assumption on the form of the functions being approximated resembles the approach by Stenger in [33], in which he also assumed that the functions being approximated belong to some predetermined regularity class. Our assumption means that our method focuses on functions $f(x)$ that are in the range of the truncated Laplace transform after the change of variable $x = e^{-s}$, with $f(e^{-s}) = \int_a^b e^{-s\mu} \sigma(\mu) d\mu$. The reciprocal-log approximation [23] shares a similar idea. This method specializes in approximating functions with branch-point singularities, such as $f(x) = x^\alpha$ on $[0, 1]$, where $\alpha > 0$, which are transformed into decaying exponentials $e^{-s\alpha}$ by the same change of variable. Their approach leverages the fact that certain rational approximations can be obtained to approximate these decaying exponentials with an exponential rate of convergence. Consequently, x^α can be approximated with an exponential rate of convergence using a rational approximation $r(s)$ with the change of variable $s = -\log x$. In contrast, our method relies on the discretization of the integral representation of $f(e^{-s})$ through the use of the singular value decomposition of the truncated Laplace transform. Our procedure yields the quadrature nodes that enable us to approximate $f(x)$ using singular powers. The methodology in [4] also bears certain similarities with our method, in that they assume implicit integral representations of the functions, with decaying exponential kernels. However, rather than directly discretizing the integrals or the integral operators, they identify the exponential terms and coefficients in their approximations through an analysis of the singular value decomposition of some Hankel matrix constructed from the function values.

Our method converges exponentially, in contrast to rational approximation which converges only at a root-exponential rate. When compared to the DE-Sinc approximation method which requires a large number of collocation points placed at the both endpoints after applying the smooth transformation (even when singularities only occur at only one endpoint), and reciprocal-log approximation which uses many collocation points together with least squares, our method has a small number of both basis functions

and collocation points, such that the coefficients can be determined via a square, low-dimensional Vandermonde-like system. Unlike the method proposed by Beylkin and Monzón [4], which only ensures an accurate approximation at equidistant points, our method ensures a small uniform error over the entire interval. Compared to expert-driven approximation, our method does not require any prior knowledge of the singularity types, besides the values of a and b , and the resulting basis functions depend only on these values, together with the precision ϵ .

The structure of this paper is as follows. Section 2 reviews the truncated Laplace transform and the truncated singular value decomposition of a matrix. Section 3 demonstrates some numerical findings about the singular value decomposition of the truncated Laplace transform. Section 4 develops the main analytical tools of this paper. Section 5 presents some numerical experiments which provide practical conditions for the use of the theorems in Section 4. Section 6 shows that functions of the form $f(x) = \int_a^b x^\mu \sigma(\mu) d\mu$ can be approximated uniformly by expansions in singular powers. Section 7 shows that the coefficients of such expansions can be obtained numerically by solving a Vandermonde-like system, and provides a bound for the uniform approximation error. Section 8 illustrates that the previous results can be extended to the case where the measure is replaced by a distribution. Section 9 describes the resulting numerical algorithm for approximating functions of the form $f(x) = \int_a^b x^\mu \sigma(\mu) d\mu$ by expansions in singular powers. Finally, Section 10 presents several numerical experiments which demonstrate the performance of our algorithm.

2 Mathematical Preliminaries

In this section, we provide some mathematical preliminaries.

2.1 The Truncated Laplace Transform

Throughout this paper, we utilize the analytical and numerical properties of the truncated Laplace transform, which have been previously presented in [17]. Here, we briefly review the key properties.

For a function $f(x) \in L^2[a, b]$, where $0 < a < b < \infty$, the truncated Laplace transform $\mathcal{L}_{a,b}$ is a linear mapping $L^2[a, b] \rightarrow L^2[0, \infty)$, defined by the formula

$$(\mathcal{L}_{a,b}(f))(x) = \int_a^b e^{-xt} f(t) dt. \quad (5)$$

We introduce the operator $T_\gamma: L^2[0, 1] \rightarrow L^2[0, \infty)$, defined by the formula

$$(T_\gamma(f))(x) = \int_0^1 e^{-x(t+\frac{1}{\gamma-1})} f(t) dt, \quad (6)$$

so that T_γ is the truncated Laplace transform shifted from $L^2[a, b]$ to $L^2[0, 1]$, where $\gamma = \frac{b}{a}$. It is clear that $\mathcal{L}_{a,b}$ and T_γ are compact operators (see, for example [3]).

As pointed out in [17], the singular value decomposition of the operator T_γ consists of an orthonormal sequence of right singular functions $\{u_i\}_{i=0,1,\dots,\infty} \in L^2[0, 1]$, an

orthonormal sequence of left singular functions $\{v_i\}_{i=0,1,\dots,\infty} \in L^2[0, \infty)$, and a discrete sequence of singular values $\{\alpha_i\}_{i=0,1,\dots,\infty} \in \mathbb{R}$. The operator T_γ can be rewritten as

$$(T_\gamma(f))(x) = \sum_{i=0}^{\infty} \alpha_i \left(\int_0^1 u_i(t) f(t) dt \right) v_i(x), \quad (7)$$

for any function $f(x) \in L^2[0, 1]$. Note that

$$T_\gamma(u_i) = \alpha_i v_i, \quad (8)$$

and

$$T_\gamma^*(v_i) = \alpha_i u_i, \quad (9)$$

for all $i = 0, 1, \dots$, where $T_\gamma^*: L^2[0, \infty) \rightarrow L^2[0, 1]$ is the adjoint of T_γ , defined by

$$(T_\gamma^*(g))(t) = \int_0^\infty e^{-x(t+\frac{1}{\gamma-1})} g(x) dx. \quad (10)$$

Similarly, T_γ^* can be rewritten as

$$(T_\gamma^*(g))(t) = \sum_{i=0}^{\infty} \alpha_i \left(\int_0^\infty v_i(x) g(x) dx \right) u_i(t). \quad (11)$$

Furthermore, for all $i = 0, 1, \dots$,

$$\alpha_i > \alpha_{i+1} \geq 0, \quad (12)$$

and the sequence $\{\alpha_i\}_{i=0,1,\dots,\infty}$ decays exponentially fast in i , where the decay rate is described in Theorem 2.2.

Assume that the left singular functions of $\mathcal{L}_{a,b}$ are denoted by $\tilde{v}_0, \tilde{v}_1, \dots$, and that the right singular functions of $\mathcal{L}_{a,b}$ are denoted by $\tilde{u}_0, \tilde{u}_1, \dots$. Then, the relations between the singular functions of $\mathcal{L}_{a,b}$ and those of T_γ are given by the formulas

$$u_i(t) = \sqrt{b-a} \tilde{u}_i(a + (b-a)t), \quad (13)$$

and

$$v_i(x) = \frac{1}{\sqrt{b-a}} \tilde{v}_i\left(\frac{x}{b-a}\right), \quad (14)$$

for all $i = 0, 1, \dots$. It is observed in [17] that $\tilde{v}_0, \tilde{v}_1, \dots$ are the eigenfunctions of the 4th order differential operator \widehat{D}_ω , defined by

$$\left(\widehat{D}_\omega(f)\right)(\omega) = -\frac{d^2}{d\omega^2} \left(\omega^2 \frac{d^2}{d\omega^2} f(\omega) \right) + (a^2 + b^2) \frac{d}{d\omega} \left(\omega^2 \frac{d}{d\omega} f(\omega) \right) + (-a^2 b^2 \omega^2 + 2a^2) f(\omega), \quad (15)$$

where $f \in C^4[0, \infty) \cap L^2[0, \infty)$, and that $\tilde{u}_0, \tilde{u}_1, \dots$ are the eigenfunctions of the 2nd order differential operator \tilde{D}_t , defined by

$$\left(\tilde{D}_t(f)\right)(t) = \frac{d}{dt} \left((t^2 - a^2)(b^2 - t^2) \frac{d}{dt} f(t) \right) - 2(t^2 - a^2) f(t), \quad (16)$$

where $f \in C^2[a, b]$. Thus, \tilde{v}_i , for all $i = 0, 1, \dots$, can be evaluated by finding the solution to the differential equation

$$-\frac{d^2}{d\omega^2} \left(\omega^2 \frac{d^2}{d\omega^2} \tilde{v}_i(\omega) \right) + (a^2 + b^2) \frac{d}{d\omega} \left(\omega^2 \frac{d}{d\omega} \tilde{v}_i(\omega) \right) + (-a^2 b^2 \omega^2 + 2a^2) \tilde{v}_i(\omega) = \hat{\chi}_i \tilde{v}_i(\omega), \quad (17)$$

where $\hat{\chi}_i$ is the i th eigenvalue of the differential operator \hat{D}_ω . Similarly, \tilde{u}_i , for all $i = 0, 1, \dots$, can be evaluated by finding the solution to the differential equation

$$\frac{d}{dt} \left((t^2 - a^2)(b^2 - t^2) \frac{d}{dt} \tilde{u}_i(t) \right) - 2(t^2 - a^2) \tilde{u}_i(t) = \tilde{\chi}_i \tilde{u}_i(t), \quad (18)$$

where $\tilde{\chi}_i$ is the i th eigenvalue of the differential operator \tilde{D}_t . It is known that the singular functions \tilde{v}_i and \tilde{u}_i (and thus v_i and u_i) have exactly i distinct roots, for all $i = 0, 1, \dots$.

A procedure for the evaluation of the singular functions and singular values of the operator T_γ is described comprehensively in [17] and [18].

The following lemma states that, for any function which is analytic and bounded within a Bernstein ellipse E_ρ , the coefficients in its Chebyshev expansion decay at an exponential rate (see Chapter 8 of [37]). We will use it to prove that the singular values $\alpha_0, \alpha_1, \dots$ of T_γ decay exponentially.

Lemma 2.1. *Let a function f analytic in $[-1, 1]$ be analytically continuable to the open Bernstein ellipse E_ρ , where it satisfies $|f(x)| \leq M$ for some M . Then its Chebyshev coefficients satisfy $|a_0| \leq M$ and*

$$|a_k| \leq 2M\rho^{-k}, \quad k \geq 1. \quad (19)$$

The following theorem demonstrates that the singular values of T_γ decay at an exponential rate, which decreases as γ increases.

Theorem 2.2. *Suppose that $\alpha_0, \alpha_1, \dots$ are the singular values of T_γ , for some $\gamma > 1$. Then, α_n decays exponentially with n , and the decay rate decreases with increasing γ . Specifically, for each $c \in (0, 1)$,*

$$\alpha_n \leq \sqrt{\frac{\gamma - 1}{(1 - c)(1 - \rho)}} \rho^{-\frac{n}{2}}, \quad (20)$$

where

$$\rho = 1 + \frac{4c}{\gamma - 1} + \sqrt{\left(\frac{4c}{\gamma - 1} \right)^2 + \frac{8c}{\gamma - 1}}. \quad (21)$$

Proof. We can view $T_{\gamma, [-1, 1]}$ as the operator T_γ shifted from $L^2[0, 1]$ to $L^2[-1, 1]$, defined by

$$(T_{\gamma, [-1, 1]}(f))(x) = \int_{-1}^1 e^{-x(\frac{t+1}{2} + \frac{1}{\gamma-1})} f(t) dt, \quad (22)$$

while its adjoint $T_{\gamma,[-1,1]}^*: L^2[0, \infty) \rightarrow L^2[-1, 1]$ is given by

$$(T_{\gamma,[-1,1]}^*(g))(t) = \int_0^\infty e^{-x(\frac{t+1}{2} + \frac{1}{\gamma-1})} g(x) dx. \quad (23)$$

It follows that the self-adjoint operator $S := T_{\gamma,[-1,1]}^* T_{\gamma,[-1,1]}: L^2[-1, 1] \rightarrow L^2[-1, 1]$ is given by

$$\begin{aligned} (S(f))(x) &= \int_0^\infty e^{-y(\frac{x+1}{2} + \frac{1}{\gamma-1})} \left[\int_{-1}^1 e^{-y(\frac{t+1}{2} + \frac{1}{\gamma-1})} f(t) dt \right] dy \\ &= \int_{-1}^1 \left[\int_0^\infty e^{-y(\frac{x+1}{2} + \frac{1}{\gamma-1})} e^{-y(\frac{t+1}{2} + \frac{1}{\gamma-1})} dy \right] f(t) dt \\ &= \int_{-1}^1 \left[\int_0^\infty e^{-y(\frac{x+t}{2} + \frac{\gamma+1}{\gamma-1})} dy \right] f(t) dt \\ &= \int_{-1}^1 \frac{2(\gamma-1)}{(x+t)(\gamma-1) + 2(\gamma+1)} f(t) dt. \end{aligned} \quad (24)$$

We now let

$$K(x, t) = \frac{2(\gamma-1)}{(x+t)(\gamma-1) + 2(\gamma+1)}, \quad (25)$$

so that

$$(S(f))(x) = \int_{-1}^1 K(x, t) f(t) dt. \quad (26)$$

Notice that, for each fixed $x \in [-1, 1]$, $K(x, t)$ has a pole at $t = -x - 2 - \frac{4}{\gamma-1} < -1$, where $\gamma \in (1, \infty)$. Thus, for each fixed $x \in [-1, 1]$, $K(x, t)$ is analytic on $[-1, 1]$, and admits an analytic continuation to a Bernstein ellipse E_ρ with the semi-major axis a , where

$$a = \frac{1}{2}(\rho + \frac{1}{\rho}). \quad (27)$$

We observe that $a = 0 - (-1 - c\frac{4}{\gamma-1}) = 1 + c\frac{4}{\gamma-1}$, for some $c \in (0, 1)$. Thus,

$$1 + c\frac{4}{\gamma-1} = \frac{1}{2}(\rho + \frac{1}{\rho}), \quad (28)$$

which implies

$$\rho = 1 + \frac{4c}{\gamma-1} \pm \sqrt{\left(\frac{4c}{\gamma-1}\right)^2 + \frac{8c}{\gamma-1}}, \quad (29)$$

where $\gamma \in (1, \infty)$. Since the definition of E_ρ assumes $\rho > 1$, we have

$$\rho = 1 + \frac{4c}{\gamma-1} + \sqrt{\left(\frac{4c}{\gamma-1}\right)^2 + \frac{8c}{\gamma-1}}, \quad (30)$$

where the parameter ρ decreases with increasing γ . It follows that $K(x, z)$ can be expanded as

$$K(x, z) = \sum_{j=0}^{\infty} a_j(x) T_j(z), \quad (31)$$

for $z \in E_\rho$. Noticing that $|K(x, z)|$ attains its maximum value when $z + x = -2 - \frac{4c}{\gamma-1}$, we have

$$\begin{aligned} |K(x, z)| &= \left| \frac{2(\gamma-1)}{(x+z)(\gamma-1) + 2(\gamma+1)} \right| \\ &\leq \left| \frac{2(\gamma-1)}{(-2 - \frac{4c}{\gamma-1})(\gamma-1) + 2(\gamma+1)} \right| \\ &= \frac{\gamma-1}{2-2c}, \end{aligned} \quad (32)$$

where $c \in (0, 1)$ and $\gamma \in (1, \infty)$, so $|K(x, z)|$ is uniformly bounded by $\frac{\gamma-1}{2-2c}$ for $x \in [-1, 1]$ and $z \in E_\rho$. Thus, Lemma 2.1 implies that

$$\sup_{-1 \leq x \leq 1} |a_j(x)| \leq \frac{\gamma-1}{1-c} \rho^{-j}, \quad (33)$$

where ρ is given by Equation (29). For each n , we let

$$K_n(x, z) = \sum_{j=0}^{n-1} a_j(x) T_j(z), \quad (34)$$

and we define $S_n: L^2[-1, 1] \rightarrow L^2[-1, 1]$ by

$$(S_n(f))(x) = \int_{-1}^1 K_n(x, t) f(t) dt. \quad (35)$$

Since the Chebyshev polynomials are bounded in uniform norm by 1 and the size of coefficients decay exponentially fast, we have

$$|K(x, z) - K_n(x, z)| = \left| \sum_{j=n}^{\infty} a_j(x) T_j(z) \right| \leq \sum_{j=n}^{\infty} |a_j(x)| \leq \frac{\gamma-1}{(1-c)(1-\rho)} \rho^{-n}. \quad (36)$$

It follows that

$$\|S - S_n\| \leq \frac{2(\gamma-1)}{(1-c)(1-\rho)} \rho^{-n}, \quad (37)$$

and we have

$$\lambda_n \leq \|S - S_n\| \leq \frac{2(\gamma-1)}{(1-c)(1-\rho)} \rho^{-n}, \quad (38)$$

where $\lambda_1 \geq \lambda_2 \geq \dots$ are the singular values of S , because the n -th singular value is the optimal error of the rank- $(n-1)$ approximation to S . Recalling that $\alpha_0 \geq \alpha_1 \geq \dots$ are

the singular values of T_γ , which are the same as the singular values of $T_{\gamma,[-1,1]}$, and they satisfy

$$2\alpha_n^2 = \lambda_n, \quad (39)$$

we have

$$\alpha_n \leq \sqrt{\frac{\gamma - 1}{(1 - c)(1 - \rho)}} \rho^{-\frac{n}{2}}. \quad (40)$$

■

2.2 The Truncated Singular Decomposition (TSVD)

The singular value decomposition (SVD) of a matrix $A \in \mathbb{R}^{m \times n}$ is defined by

$$A = U \Sigma V^T, \quad (41)$$

where the left and right matrices $U \in \mathbb{R}^{m \times m}$ and $V \in \mathbb{R}^{n \times n}$ are orthogonal, and the matrix $\Sigma \in \mathbb{R}^{m \times n}$ is a diagonal matrix with the singular values of A on the diagonal, in descending order, so that

$$\Sigma = \text{diag}(\sigma_1, \sigma_2, \dots, \sigma_{\min\{m,n\}}). \quad (42)$$

Let $r \leq \min\{m, n\}$ denote the rank of A , which is equal to the number of nonzero entries on the diagonal, and suppose that $k \leq r$. The k -truncated singular value decomposition (k -TSVD) of A is defined as

$$A_k = U \Sigma_k V^T, \quad (43)$$

where

$$\Sigma_k = \text{diag}(\sigma_1, \dots, \sigma_k, 0, \dots, 0) \in \mathbb{R}^{m \times n}. \quad (44)$$

The pseudo-inverse of A_k is defined by

$$A_k^\dagger = V \Sigma_k^\dagger U^T \in \mathbb{R}^{n \times m}, \quad (45)$$

where

$$\Sigma_k^\dagger = \text{diag}(\sigma_1^{-1}, \dots, \sigma_k^{-1}, 0, \dots, 0) \in \mathbb{R}^{n \times m}. \quad (46)$$

The following theorem bounds the sizes of the solution and residual, when a perturbed linear system is solved using the TSVD. It follows the same reasoning as the proof of Theorem 3.4 in [14], and can be viewed as a more explicit version of Lemma 3.3 in [6].

Theorem 2.3. *Suppose that $A \in \mathbb{R}^{m \times n}$, where $m \geq n$, and let $\sigma_1 \geq \sigma_2 \geq \dots \geq \sigma_n$ be the singular values of A . Let $b \in \mathbb{R}^m$, and suppose that $x \in \mathbb{R}^n$ satisfies*

$$Ax = b. \quad (47)$$

Let $\epsilon > 0$, and suppose further that

$$\widehat{x}_k = (A + E)_k^\dagger(b + e), \quad (48)$$

where $(A + E)_k^\dagger$ is the pseudo-inverse of the k -TSVD of $A + E$, so that

$$\widehat{\sigma}_k \geq \epsilon \geq \widehat{\sigma}_{k+1}, \quad (49)$$

where $\widehat{\sigma}_k$ and $\widehat{\sigma}_{k+1}$ are the k th and $(k + 1)$ th largest singular values of $A + E$, defining $\widehat{\sigma}_{n+1} := 0$, and where $E \in \mathbb{R}^{m \times n}$ and $e \in \mathbb{R}^m$, with $\|E\|_2 < \epsilon/2$. Then

$$\|\widehat{x}_k\|_2 \leq \frac{1}{\widehat{\sigma}_k}(2\epsilon\|x\|_2 + \|e\|_2) + \|x\|_2 \quad (50)$$

and

$$\|A\widehat{x}_k - b\|_2 \leq 5\epsilon\|x\|_2 + \frac{3}{2}\|e\|_2. \quad (51)$$

Proof. Let $\sigma_1 \geq \sigma_2 \geq \dots \geq \sigma_n$ denote the singular values of A , and let A_k be the k -TSVD of A . We observe that $A_k x = b - (A - A_k)x$. Letting $r_k = (A - A_k)x$ denote the residual, we see that $\|r_k\|_2 \leq \sigma_{k+1}\|x\|_2$ and that $b - A_k x = r_k$, defining $\sigma_{n+1} := 0$. Let $x_k = A_k^\dagger b$. Clearly, $b - Ax_k = r_k$ and $\|x_k\|_2 \leq \|x\|_2$.

Let $\widehat{A} := A + E$. We see that

$$\begin{aligned} \widehat{x}_k &= \widehat{A}_k^\dagger(b + e) \\ &= \widehat{A}_k^\dagger(Ax_k + r_k + e) \\ &= \widehat{A}_k^\dagger(\widehat{A}x_k - Ex_k + r_k + e) \\ &= \widehat{A}_k^\dagger(-Ex_k + r_k + e) + \widehat{A}_k^\dagger\widehat{A}x_k \\ &= \widehat{A}_k^\dagger(-Ex_k + r_k + e) + \widehat{A}_k^\dagger\widehat{A}_k x_k. \end{aligned} \quad (52)$$

Taking norms on both sides and observing that $\widehat{A}_k^\dagger\widehat{A}_k$ is an orthogonal projection,

$$\begin{aligned} \|\widehat{x}_k\|_2 &\leq \|\widehat{A}_k^\dagger\|_2(\|E\|_2\|x_k\|_2 + \|e\|_2 + \|r_k\|_2) + \|x_k\|_2 \\ &\leq \|\widehat{A}_k^\dagger\|_2(\|E\|_2\|x_k\|_2 + \|e\|_2 + \sigma_{k+1}\|x\|_2) + \|x_k\|_2. \end{aligned} \quad (53)$$

Letting $\widehat{\sigma}_1 \geq \widehat{\sigma}_2 \geq \dots \geq \widehat{\sigma}_n$ denote the singular values of $A + E$, we have by the Bauer-Fike Theorem (see [2]) that $|\widehat{\sigma}_j - \sigma_j| \leq \|E\|_2$ for $j = 1, 2, \dots, n$. Since $\widehat{\sigma}_k \geq \epsilon \geq \widehat{\sigma}_{k+1}$ and $\|E\|_2 < \epsilon/2$, we see that $\sigma_{k+1} < 3\epsilon/2$. Therefore,

$$\begin{aligned} \|\widehat{x}_k\|_2 &\leq \frac{1}{\widehat{\sigma}_k}\left(\frac{\epsilon}{2}\|x\|_2 + \|e\|_2 + \frac{3\epsilon}{2}\|x\|_2\right) + \|x\|_2 \\ &= \frac{1}{\widehat{\sigma}_k}(2\epsilon\|x\|_2 + \|e\|_2) + \|x\|_2. \end{aligned} \quad (54)$$

To bound the residual, we observe that

$$\begin{aligned} A\widehat{x}_k - b &= A\widehat{x}_k - Ax_k - r_k \\ &= A(\widehat{x}_k - x_k) - r_k \\ &= \widehat{A}(\widehat{x}_k - x_k) - E(\widehat{x}_k - x_k) - r_k. \end{aligned} \quad (55)$$

From Equation (52), we have that

$$\widehat{x}_k - x_k = \widehat{A}_k^\dagger(-Ex_k + r_k + e) - (I - \widehat{A}_k^\dagger \widehat{A}_k)x_k. \quad (56)$$

Combining these two formulas,

$$\begin{aligned} A\widehat{x}_k - b &= \widehat{A}\widehat{A}_k^\dagger(-Ex_k + r_k + e) - \widehat{A}(I - \widehat{A}_k^\dagger \widehat{A}_k)x_k - E(\widehat{x}_k - x_k) - r_k \\ &= \widehat{A}_k \widehat{A}_k^\dagger(-Ex_k + r_k + e) - \widehat{A}(I - \widehat{A}_k^\dagger \widehat{A}_k)x_k - E(\widehat{x}_k - x_k) - r_k \\ &= \widehat{A}_k \widehat{A}_k^\dagger(-Ex_k + e) - \widehat{A}(I - \widehat{A}_k^\dagger \widehat{A}_k)x_k - E(\widehat{x}_k - x_k) - (I - \widehat{A}_k \widehat{A}_k^\dagger)r_k. \end{aligned} \quad (57)$$

Since $\widehat{A}(I - \widehat{A}_k^\dagger \widehat{A}_k) = (\widehat{A} - \widehat{A}_k)(I - \widehat{A}_k^\dagger \widehat{A}_k)$, we see that

$$A\widehat{x}_k - b = \widehat{A}_k \widehat{A}_k^\dagger(-Ex_k + e) - (\widehat{A} - \widehat{A}_k)(I - \widehat{A}_k^\dagger \widehat{A}_k)x_k - E(\widehat{x}_k - x_k) - (I - \widehat{A}_k \widehat{A}_k^\dagger)r_k. \quad (58)$$

Taking norms on both sides and observing that $\widehat{A}_k \widehat{A}_k^\dagger$ and $(I - \widehat{A}_k^\dagger \widehat{A}_k)$ are orthogonal projections,

$$\begin{aligned} \|A\widehat{x}_k - b\|_2 &\leq 2\|E\|_2\|x_k\|_2 + \|e\|_2 + \widehat{\sigma}_{k+1}\|x_k\|_2 + \|E\|_2\|\widehat{x}_k\|_2 + \|r_k\|_2 \\ &\leq \frac{7}{2}\epsilon\|x\|_2 + \|e\|_2 + \frac{1}{2}\epsilon\|\widehat{x}_k\|_2 \\ &\leq 5\epsilon\|x\|_2 + \frac{3}{2}\|e\|_2. \end{aligned} \quad (59)$$

■

3 Numerical Tools

In this section, we present several numerical experiments examining some numerical properties of the singular value decomposition of the shifted truncated Laplace transform, T_γ . We make the following observations:

1. Note that the singular values of T_γ decay exponentially, with the decay rate decreasing as γ increases, as suggested by Theorem 2.2. The numerical experiments illustrated in Figure 1 show that the singular values decay at a much greater rate than the bound provided in Theorem 2.2.
2. Figures 2a, 2b and 4a show that the L^∞ -norms of both the left and right singular functions and the L^1 -norm of the left singular functions are small, for $\gamma \in [2, 1250]$.
3. Suppose that x_1, x_2, \dots, x_n are the roots of $v_n(x)$, and that t_1, t_2, \dots, t_n are the roots of $u_n(t)$. Let the weights w_1, w_2, \dots, w_n and $\widetilde{w}_1, \widetilde{w}_2, \dots, \widetilde{w}_n$ satisfy

$$\int_0^\infty v_i(x) dx = \sum_{k=1}^n w_k v_i(x_k), \quad (60)$$

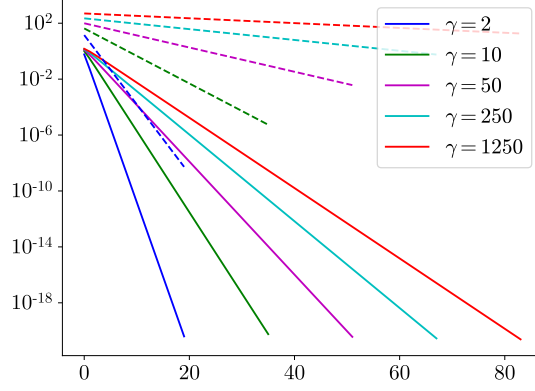


Figure 1: The singular values α_n of T_γ , as a function of n . The dashed lines indicate the bound defined in Theorem 2.2 with $c = 0.99$, for the corresponding values of γ .

and

$$\int_0^1 u_i(t) dt = \sum_{k=1}^n \tilde{w}_k u_i(t_k), \quad (61)$$

for all $i = 0, 1, \dots, n-1$. Then the weights are all positive. Moreover, Figures 3a and 4b show that $\max_{1 \leq k \leq n} \sqrt{w_k}$ and $\|\tilde{w}\|_1$ are small, for $\gamma \in [2, 1250]$.

4. Let

$$A_n^\infty := \sum_{i=n}^{\infty} \alpha_i \|v_i\|_{L^\infty[0,\infty)} \|u_i\|_{L^\infty[0,1]}, \quad (62)$$

$$A_n^1 := \sum_{i=n}^{\infty} \alpha_i \|v_i\|_{L^1[0,\infty)} \|u_i\|_{L^1[0,1]}, \quad (63)$$

$$A_n^{1,\infty} := \sum_{i=n}^{\infty} \alpha_i \|v_i\|_{L^1[0,\infty)} \|u_i\|_{L^\infty[0,1]}, \quad (64)$$

$$A_n^{\infty,1} := \sum_{i=n}^{\infty} \alpha_i \|v_i\|_{L^\infty[0,\infty)} \|u_i\|_{L^1[0,1]}, \quad (65)$$

$$U_n := \sum_{i=0}^{n-1} \|u_i\|_{L^\infty[0,1]}, \quad (66)$$

$$V_n := \sum_{i=0}^{n-1} \|v_i\|_{L^\infty[0,\infty)}. \quad (67)$$

Numerical experiments illustrated in Figures 1 to 4 imply that A_n^∞ , A_n^1 , $A_n^{1,\infty}$, and $A_n^{\infty,1}$ are approximately equal to α_n and that U_n and V_n are small. Moreover, we observe that $A_n^{\infty,1} \|w\|_1 \approx \alpha_n \|v_n\|_{L^\infty[0,\infty)} \|w\|_1$, and the size of $\|v_n\|_{L^\infty[0,\infty)} \|w\|_1$ is illustrated in Figure 3b.

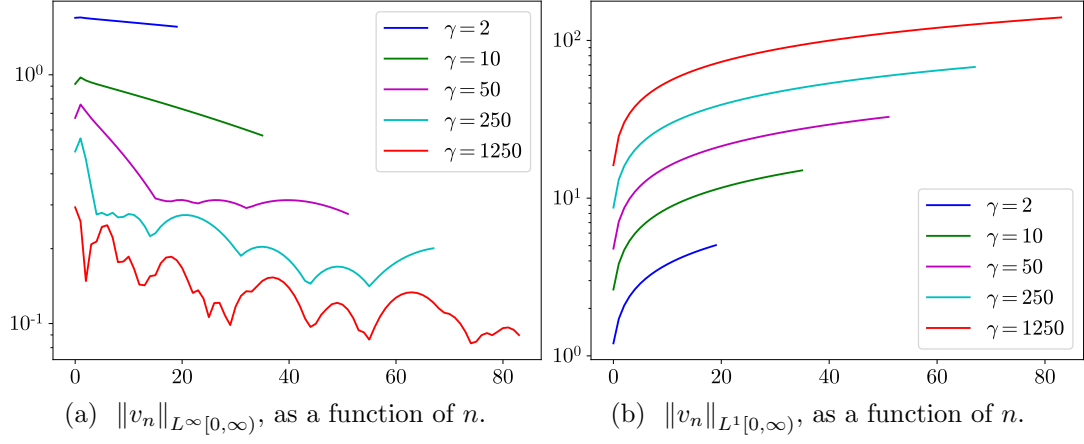


Figure 2

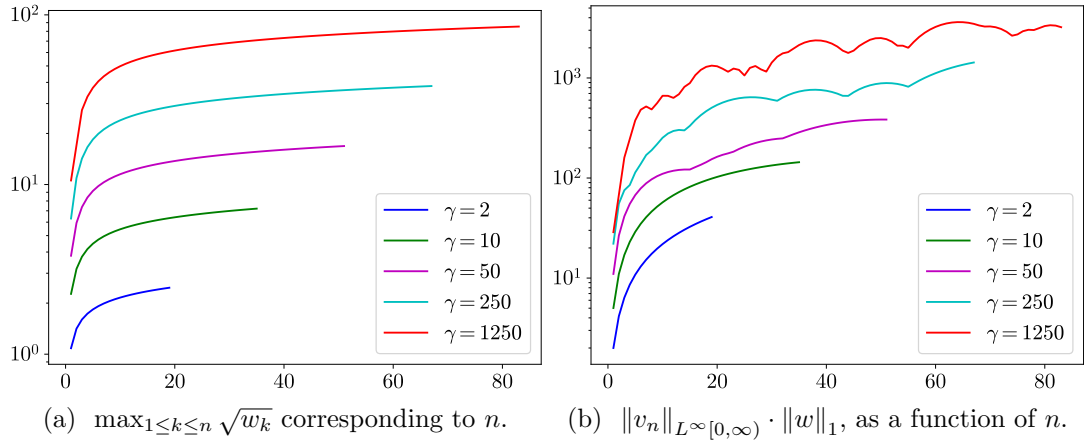


Figure 3

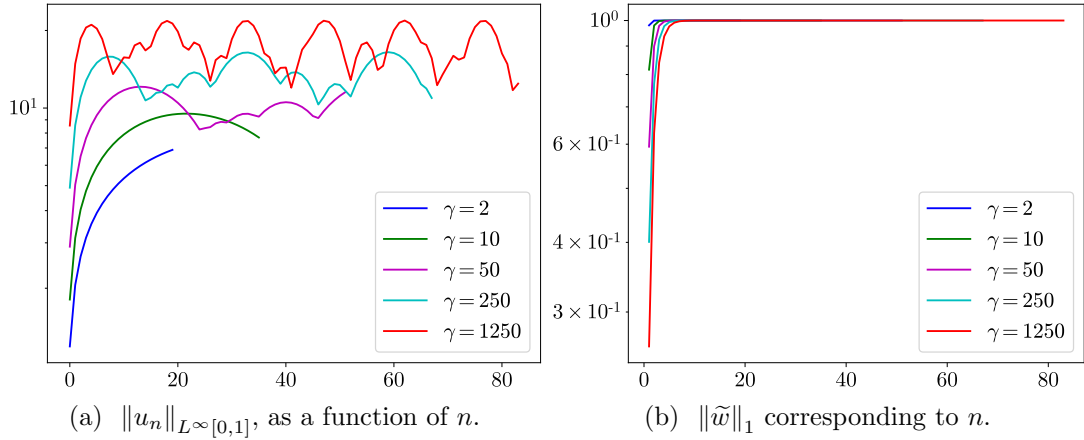


Figure 4

4 Analytical Tools

In this section, we present the principal analytical tools of this paper.

The following theorem states that the product of any two functions in the range of the operator T_γ , introduced in Section 2.1, can be expressed as T_γ applied to some $L^\infty[0, 1]$ function, after a change of variable. This result directly follows from the definition of the truncated Laplace transform.

Theorem 4.1. *Suppose that the functions $p, q \in L^2[0, \infty)$ are defined by*

$$p(x) = \int_0^1 e^{-x(t+\frac{1}{\gamma-1})} \eta(t) dt, \quad (68)$$

and

$$q(x) = \int_0^1 e^{-x(t+\frac{1}{\gamma-1})} \varphi(t) dt, \quad (69)$$

respectively, for some $\eta, \varphi \in L^2[0, 1]$, and some $\gamma > 1$. Then, there exists a $\sigma \in L^\infty[0, 1]$, such that

$$p(x) \cdot q(x) = \int_0^1 e^{-x(2t+\frac{2}{\gamma-1})} \sigma(t) dt. \quad (70)$$

Proof. For any p and q defined by Equation (68) and Equation (69), we have

$$\begin{aligned} p(x) \cdot q(x) &= \int_0^1 e^{-x(t+\frac{1}{\gamma-1})} \eta(t) dt \int_0^1 e^{-x(s+\frac{1}{\gamma-1})} \varphi(s) ds \\ &= \int_0^1 \int_0^1 e^{-x(t+s+\frac{2}{\gamma-1})} \eta(t) \varphi(s) ds dt. \end{aligned} \quad (71)$$

Defining a new variable $u = t + s$ and changing the range of integration, Equation (71) becomes

$$\begin{aligned} p(x) \cdot q(x) &= \int_0^1 e^{-x(u+\frac{2}{\gamma-1})} \int_0^u \eta(u-s) \varphi(s) ds du \\ &\quad + \int_1^2 e^{-x(u+\frac{2}{\gamma-1})} \int_{u-1}^1 \eta(u-s) \varphi(s) ds du. \end{aligned} \quad (72)$$

Letting $v = \frac{u}{2}$, we have

$$\begin{aligned} p(x) \cdot q(x) &= \int_0^{\frac{1}{2}} e^{-x(2v+\frac{2}{\gamma-1})} \int_0^{2v} \eta(2v-s) \varphi(s) ds 2dv \\ &\quad + \int_{\frac{1}{2}}^1 e^{-x(2v+\frac{2}{\gamma-1})} \int_{2v-1}^1 \eta(2v-s) \varphi(s) ds 2dv \\ &= \int_0^1 e^{-x(2v+\frac{2}{\gamma-1})} \sigma(v) dv, \end{aligned} \quad (73)$$

where

$$\sigma(v) = 2 \int_0^{2v} \eta(2v-s) \varphi(s) ds, \quad (74)$$

for $v \in [0, \frac{1}{2}]$, and

$$\sigma(v) = 2 \int_{2v-1}^1 \eta(2v-s) \varphi(s) ds, \quad (75)$$

for $v \in [\frac{1}{2}, 1]$. ■

Observation 4.1. Suppose we have nodes x_1, x_2, \dots, x_n and weights w_1, w_2, \dots, w_n , such that

$$\left| \int_0^\infty \int_0^1 e^{-x(t+\frac{1}{\gamma-1})} \eta(t) dt dx - \sum_{j=1}^n w_j \int_0^1 e^{-x_j(t+\frac{1}{\gamma-1})} \eta(t) dt \right| \leq \epsilon \|\eta\|_{L^\infty[0,1]}, \quad (76)$$

for any $\eta \in L^\infty[0,1]$. Notice that

$$\begin{aligned} & \int_0^\infty p(x) \cdot q(x) dx \\ &= \int_0^\infty p\left(\frac{u}{2}\right) \cdot q\left(\frac{u}{2}\right) \cdot \frac{1}{2} du \\ &= \int_0^\infty \frac{1}{2} \int_0^1 e^{-u(t+\frac{1}{\gamma-1})} \sigma(t) dt du. \end{aligned} \quad (77)$$

Thus,

$$\left| \int_0^\infty p(x) \cdot q(x) dx - \sum_{j=1}^n \frac{w_j}{2} \cdot p\left(\frac{x_j}{2}\right) \cdot q\left(\frac{x_j}{2}\right) \right| \leq \frac{1}{2} \epsilon \|\sigma\|_{L^\infty[0,1]} \leq \epsilon \|\eta\|_{L^2[0,1]} \|\varphi\|_{L^2[0,1]}. \quad (78)$$

The following theorem shows that the product of any two functions in the range of T_γ^* can be expressed as T_γ^* applied to some $L^\infty[0, \infty)$ function.

Theorem 4.2. Suppose that the functions $p, q \in L^2[0, 1]$ are defined by

$$p(t) = \int_0^\infty e^{-x(t+\frac{1}{\gamma-1})} \eta(x) dx, \quad (79)$$

and

$$q(t) = \int_0^\infty e^{-x(t+\frac{1}{\gamma-1})} \varphi(x) dx, \quad (80)$$

respectively, for some $\eta, \varphi \in L^2[0, \infty)$, and some $\gamma > 1$. Then, there exists a $\sigma \in L^\infty[0, \infty)$, such that

$$p(t) \cdot q(t) = \int_0^\infty e^{-x(t+\frac{1}{\gamma-1})} \sigma(x) dx. \quad (81)$$

Proof. For any p and q defined by Equation (79) and Equation (80), we have

$$\begin{aligned} p(t) \cdot q(t) &= \int_0^\infty e^{-\omega(t+\frac{1}{\gamma-1})} \eta(\omega) d\omega \int_0^\infty e^{-x(t+\frac{1}{\gamma-1})} \varphi(x) dx \\ &= \int_0^\infty \int_0^\infty e^{-(\omega+x)(t+\frac{1}{\gamma-1})} \eta(\omega) \varphi(x) dx d\omega. \end{aligned} \quad (82)$$

Defining $u = \omega + x$ and changing the range of integration, Equation (82) becomes

$$\begin{aligned} p(t) \cdot q(t) &= \int_0^\infty e^{-u(t+\frac{1}{\gamma-1})} \int_0^u \eta(\omega) \varphi(u-\omega) d\omega du \\ &= \int_0^\infty e^{-u(t+\frac{1}{\gamma-1})} \sigma(u) du, \end{aligned} \quad (83)$$

where

$$\sigma(u) = \int_0^u \eta(\omega) \varphi(u-\omega) d\omega, \quad (84)$$

for $u \in [0, \infty)$. ■

Observation 4.2. Suppose we have nodes t_1, t_2, \dots, t_n and weights $\tilde{w}_1, \tilde{w}_2, \dots, \tilde{w}_n$, such that

$$\left| \int_0^1 \int_0^\infty e^{-x(t+\frac{1}{\gamma-1})} \eta(x) dx dt - \sum_{j=1}^n \tilde{w}_j \int_0^\infty e^{-x(t_j+\frac{1}{\gamma-1})} \eta(x) dx \right| \leq \epsilon \|\eta\|_{L^\infty[0,\infty)}, \quad (85)$$

for any $\eta \in L^\infty[0, \infty)$. Since

$$p(t) \cdot q(t) = \int_0^\infty e^{-x(t+\frac{1}{\gamma-1})} \sigma(x) dx, \quad (86)$$

we have

$$\left| \int_0^1 p(t) \cdot q(t) dt - \sum_{j=1}^n \tilde{w}_j \cdot p(t_j) \cdot q(t_j) \right| \leq \epsilon \|\sigma\|_{L^\infty[0,\infty)} \leq \epsilon \|\eta\|_{L^2[0,\infty)} \|\varphi\|_{L^2[0,\infty)}. \quad (87)$$

Leveraging the multiplication rule established earlier, we demonstrate that the following quadrature rule accurately integrates the products of the kernel of T_γ and the right singular functions of T_γ .

Corollary 4.3. Suppose that we have a quadrature rule to integrate $\alpha_i u_i \cdot \alpha_j u_j$ to within an error of ϵ , for all $i, j = 0, 1, \dots, n-1$. Suppose further that t_1, t_2, \dots, t_m are the quadrature nodes, and $\tilde{w}_1, \tilde{w}_2, \dots, \tilde{w}_m$ are the quadrature weights. Then, the error of the quadrature rule applied to functions of the form $f(t) = e^{-x(t+\frac{1}{\gamma-1})} u_i(t)$, with $x \in [0, \infty)$, is bounded by

$$\frac{\epsilon}{\alpha_i} V_n + A_n^\infty \|u_i\|_{L^\infty[0,1]} \|\tilde{w}\|_1, \quad (88)$$

where V_n and A_n^∞ are defined in Equation (67) and Equation (62), respectively.

Proof. Since $e^{-x(t+\frac{1}{\gamma-1})}$ can be written as

$$e^{-x(t+\frac{1}{\gamma-1})} = \sum_{j=0}^\infty v_j(x) \alpha_j u_j(t), \quad (89)$$

we have

$$\begin{aligned}
& \left| \int_0^1 e^{-x(t+\frac{1}{\gamma-1})} u_i(t) dt - \sum_{k=1}^m \tilde{w}_k e^{-x(t_k+\frac{1}{\gamma-1})} u_i(t_k) \right| \\
&= \left| \int_0^1 \left(\sum_{j=0}^{\infty} v_j(x) \alpha_j u_j(t) \right) u_i(t) dt - \sum_{k=1}^m \tilde{w}_k \left(\sum_{j=0}^{\infty} v_j(x) \alpha_j u_j(t_k) \right) u_i(t_k) \right| \\
&= \left| \sum_{j=0}^{n-1} \int_0^1 v_j(x) \alpha_j u_j(t) u_i(t) dt + \sum_{j=n}^{\infty} \int_0^1 v_j(x) \alpha_j u_j(t) u_i(t) dt \right. \\
&\quad \left. - \sum_{j=0}^{n-1} \left(\sum_{k=1}^m \tilde{w}_k v_j(x) \alpha_j u_j(t_k) \right) u_i(t_k) - \sum_{j=n}^{\infty} \left(\sum_{k=1}^m \tilde{w}_k v_j(x) \alpha_j u_j(t_k) \right) u_i(t_k) \right| \\
&= \left| \sum_{j=0}^{n-1} \int_0^1 v_j(x) \alpha_j u_j(t) u_i(t) dt - \sum_{j=0}^{n-1} \left(\sum_{k=1}^m \tilde{w}_k v_j(x) \alpha_j u_j(t_k) \right) u_i(t_k) \right. \\
&\quad \left. - \sum_{j=n}^{\infty} \left(\sum_{k=1}^m \tilde{w}_k v_j(x) \alpha_j u_j(t_k) \right) u_i(t_k) \right| \\
&\leq \sum_{j=0}^{n-1} |v_j(x)| \cdot \frac{\epsilon}{\alpha_i} + \left| \sum_{k=1}^m \tilde{w}_k u_i(t_k) \left(\sum_{j=n}^{\infty} v_j(x) \alpha_j u_j(t_k) \right) \right| \\
&\leq \frac{\epsilon}{\alpha_i} V_n + A_n^\infty \|u_i\|_{L^\infty[0,1]} \|\tilde{w}\|_1. \tag{90}
\end{aligned}$$

■

Suppose that x_1, x_2, \dots, x_m and w_1, w_2, \dots, w_m are the nodes and weights of a quadrature rule which integrates $\alpha_i v_i \cdot \alpha_j v_j$, to within an error of ϵ , for all $i, j = 0, 1, \dots, n-1$. The following theorem shows that, if the left singular functions $\{v_i\}_{i=0,1,\dots,n-1}$ of the operator T_γ , are used as interpolation basis, then, the interpolation matrix for the nodes x_1, x_2, \dots, x_m is well conditioned, provided that the maximum error ϵ of integrating $\alpha_i v_i \cdot \alpha_j v_j$, for $i, j = 0, 1, \dots, n-1$, is sufficiently small.

Theorem 4.4. *Suppose that we have an m -point quadrature rule which integrates $\alpha_i v_i \cdot \alpha_j v_j$, to within an error of ϵ , for all $i, j = 0, 1, \dots, n-1$. Suppose further that x_1, x_2, \dots, x_m are the quadrature nodes, and w_1, w_2, \dots, w_m are the quadrature weights. Let the matrix $A \in \mathbb{R}^{m \times n}$ be given by the formula*

$$A = \begin{pmatrix} v_0(x_1) & v_1(x_1) & \dots & v_{n-1}(x_1) \\ v_0(x_2) & v_1(x_2) & \dots & v_{n-1}(x_2) \\ \vdots & \vdots & \ddots & \vdots \\ v_0(x_m) & v_1(x_m) & \dots & v_{n-1}(x_m) \end{pmatrix}, \tag{91}$$

and let the matrix W be the diagonal matrix with diagonal entries w_1, w_2, \dots, w_m . We define the matrix $E = [e_{jk}]$ such that

$$E = I - A^T W A. \tag{92}$$

Then,

$$|e_{jk}| \leq \frac{\epsilon}{\alpha_{j-1} \alpha_{k-1}}. \tag{93}$$

Proof. From Equation (92), we have

$$e_{jk} = \delta_{jk} - \sum_{l=1}^m w_l v_{j-1}(x_l) v_{k-1}(x_l), \quad (94)$$

where $\delta_{jk} = 1$ if $j = k$, and $\delta_{jk} = 0$ otherwise. Then,

$$\begin{aligned} |e_{jk}| &= \left| \delta_{jk} - \sum_{l=1}^m w_l \alpha_{j-1} v_{j-1}(x_l) \cdot \alpha_{k-1} v_{k-1}(x_l) \frac{1}{\alpha_{j-1} \alpha_{k-1}} \right| \\ &\leq \left| \delta_{jk} - \frac{1}{\alpha_{j-1} \alpha_{k-1}} \int_0^\infty \alpha_{j-1} v_{j-1}(x) \cdot \alpha_{k-1} v_{k-1}(x) dx \right| + \frac{\epsilon}{\alpha_{j-1} \alpha_{k-1}} \\ &= \frac{\epsilon}{\alpha_{j-1} \alpha_{k-1}}. \end{aligned} \quad (95)$$

■

The following corollary establishes an upper bound on the norm of the pseudo-inverse A^\dagger of the matrix A defined in Equation (91).

Corollary 4.5. *Suppose that we have a collection of quadrature nodes x_1, x_2, \dots, x_m and positive quadrature weights w_1, w_2, \dots, w_m , which integrates $\alpha_i v_i \cdot \alpha_j v_j$ to within an error of $\epsilon \leq \frac{\alpha_n^2}{2n}$, for all $i, j = 0, 1, \dots, n-1$. Let $A \in \mathbb{R}^{m \times n}$ be the matrix defined in Equation (91). Then,*

$$\|A^\dagger\|_2 < \sqrt{2} \max_{1 \leq i \leq m} \sqrt{w_i}, \quad (96)$$

where $A^\dagger \in \mathbb{R}^{n \times m}$ is the pseudo-inverse of A .

Proof. Recalling that w_1, w_2, \dots, w_m are positive, we let $W^{\frac{1}{2}}$ denote a diagonal matrix with entries $\sqrt{w_1}, \sqrt{w_2}, \dots, \sqrt{w_m}$. We define B such that $B = W^{\frac{1}{2}} A$. It follows from Equation (92) that $B^T B = I - E$. Since $e_{jk} < \frac{\epsilon}{\alpha_n^2}$, for all $j, k = 1, 2, \dots, n$, we have $\|E\|_2 < \frac{\epsilon}{\alpha_n^2} n$. Let $\tilde{\sigma}_1, \tilde{\sigma}_2, \dots, \tilde{\sigma}_n$ denote the singular values of $B^T B$. Then, it can be shown that (see Theorem IIIa in [2])

$$|\tilde{\sigma}_j - 1| \leq \|E\|_2 < \frac{\epsilon}{\alpha_n^2} n, \quad (97)$$

for all $j = 1, 2, \dots, n$. This means that

$$1 - \frac{\epsilon}{\alpha_n^2} n < \tilde{\sigma}_j < 1 + \frac{\epsilon}{\alpha_n^2} n. \quad (98)$$

Letting $k = \min\{n, m\}$ and $\sigma_1, \sigma_2, \dots, \sigma_k$ be the singular values of B , we have

$$\sqrt{1 - \frac{\epsilon}{\alpha_n^2} n} < \sigma_j < \sqrt{1 + \frac{\epsilon}{\alpha_n^2} n}. \quad (99)$$

Letting B^\dagger be the pseudo-inverse of B , such that $B^\dagger B = I$, since $B = W^{\frac{1}{2}} A$, we have that $A^\dagger = B^\dagger W^{\frac{1}{2}}$. Thus,

$$\begin{aligned} \|A^\dagger\|_2 &\leq \|B^\dagger\|_2 \|W^{\frac{1}{2}}\|_2 \\ &< \frac{1}{\sqrt{1 - \frac{\epsilon}{\alpha_n^2} n}} \cdot \max_{1 \leq i \leq m} \sqrt{w_i}. \end{aligned} \quad (100)$$

If we have $\epsilon \leq \frac{\alpha_n^2}{2n}$, then Equation (100) implies that

$$\|A^\dagger\|_2 < \sqrt{2} \max_{1 \leq i \leq m} \sqrt{w_i}. \quad (101)$$

■

5 Selecting the Quadrature Nodes and Weights

In this section, we discuss how to construct the quadrature rules described in the conditions of the theorems presented in Section 4.

Suppose that the nodes t_1, t_2, \dots, t_m are the roots of $u_m(t)$, and that the weights $\tilde{w}_1, \tilde{w}_2, \dots, \tilde{w}_m$ satisfy

$$\int_0^1 u_i(t) dt = \sum_{k=1}^m \tilde{w}_k u_i(t_k), \quad (102)$$

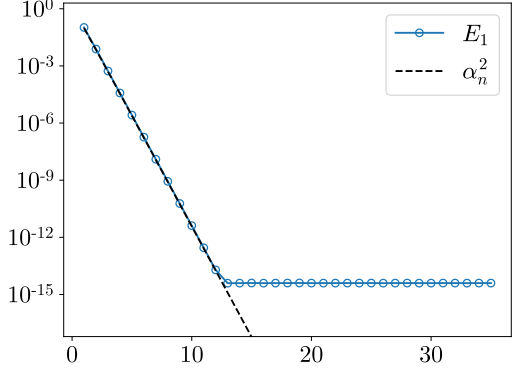
for all $i = 0, 1, \dots, m-1$. Then, Equation (11) and Equation (102) imply that

$$\begin{aligned} & \left| \int_0^1 \int_0^\infty e^{-x(t+\frac{1}{\gamma-1})} \eta(x) dx dt - \sum_{k=1}^m \tilde{w}_k \int_0^\infty e^{-x(t_k+\frac{1}{\gamma-1})} \eta(x) dx \right| \\ &= \left| \int_0^1 \sum_{i=0}^\infty \alpha_i \left(\int_0^\infty v_i(x) \eta(x) dx \right) u_i(t) dt - \sum_{k=1}^m \tilde{w}_k \sum_{i=0}^\infty \alpha_i \left(\int_0^\infty v_i(x) \eta(x) dx \right) u_i(t_k) \right| \\ &= \left| \int_0^1 \sum_{i=m}^\infty \alpha_i \left(\int_0^\infty v_i(x) \eta(x) dx \right) u_i(t) dt - \sum_{k=1}^m \tilde{w}_k \sum_{i=m}^\infty \alpha_i \left(\int_0^\infty v_i(x) \eta(x) dx \right) u_i(t_k) \right| \\ &\leq \left| \int_0^1 \sum_{i=m}^\infty \alpha_i \left(\int_0^\infty v_i(x) \eta(x) dx \right) u_i(t) dt \right| + \left| \sum_{k=1}^m \tilde{w}_k \sum_{i=m}^\infty \alpha_i \left(\int_0^\infty v_i(x) \eta(x) dx \right) u_i(t_k) \right| \\ &\leq \|\eta\|_{L^\infty[0,\infty)} (A_m^1 + A_m^{1,\infty} \|\tilde{w}\|_1), \end{aligned} \quad (103)$$

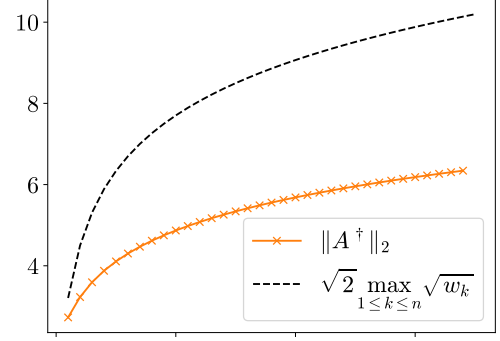
where A_m^1 and $A_m^{1,\infty}$ are defined in Equation (63) and Equation (64), respectively. It follows from Observation 4.2 that

$$E_1 := \max_{0 \leq i, j \leq n-1} \left| \int_0^1 \alpha_i u_i(t) \cdot \alpha_j u_j(t) dt - \sum_{k=1}^m \tilde{w}_k \alpha_i u_i(t_k) \cdot \alpha_j u_j(t_k) \right| \leq A_m^1 + A_m^{1,\infty} \|\tilde{w}\|_1. \quad (104)$$

Since $A_m^1 \approx \alpha_m$, $A_m^{1,\infty} \approx \alpha_m$, and $\|\tilde{w}\|_1$ is small, we have $E_1 \lesssim \alpha_m$. If $E_1 \leq \alpha_n^2$, then Corollary 4.3 guarantees that such a quadrature rule integrates the functions $f(t) = e^{-x(t+\frac{1}{\gamma-1})} u_i(t)$, for $i = 0, 1, \dots, n-1$, to an error of approximately the same size as α_n . Since the singular values α_i decay exponentially, we see that $E_1 \lesssim \alpha_m \leq \alpha_n^2$ when $m \approx 2n$. In practice, however, it is unnecessary to take m to be so large. Numerical experiments for $\gamma = 10, 50$ and 250 demonstrate that, by choosing $m = n$, the error of the quadrature rule applied to $\alpha_i u_i \cdot \alpha_j u_j$, for all $i, j = 0, 1, \dots, n-1$, turns out to be smaller than α_n^2 , as shown in Figures 5a, 6a and 7a. Thus, it follows from Corollary 4.3

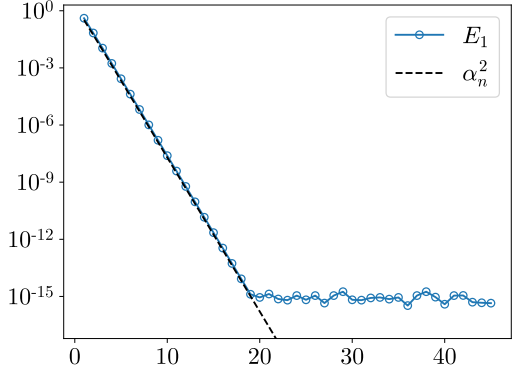


(a) A comparison between E_1 and α_n^2 , as a function of n , where $m = n$.

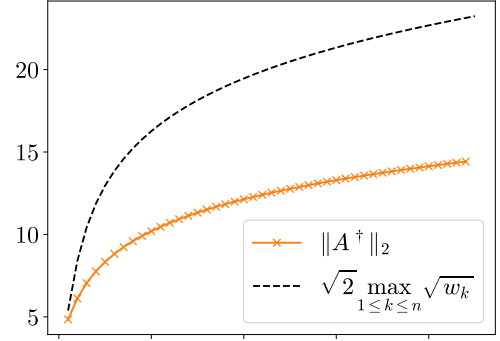


(b) A comparison between $\|A^\dagger\|_2$ and $\sqrt{2} \max_k \sqrt{w_k}$, as a function of n , where $m = n$.

Figure 5: $\gamma = 10$



(a) A comparison between E_1 and α_n^2 , as a function of n , where $m = n$.



(b) A comparison between $\|A^\dagger\|_2$ and $\sqrt{2} \max_k \sqrt{w_k}$, as a function of n , where $m = n$.

Figure 6: $\gamma = 50$

that the error of the quadrature rule applied to $f(t) = e^{-x(t+\frac{1}{\gamma-1})} u_i(t)$, for $i = 0, 1, \dots, n-1$, is approximately α_n .

Suppose now that the nodes x_1, x_2, \dots, x_m are the roots of $v_m(x)$, and the weights w_1, w_2, \dots, w_m satisfy

$$\int_0^\infty v_i(x) dx = \sum_{k=1}^m w_k v_i(x_k), \quad (105)$$

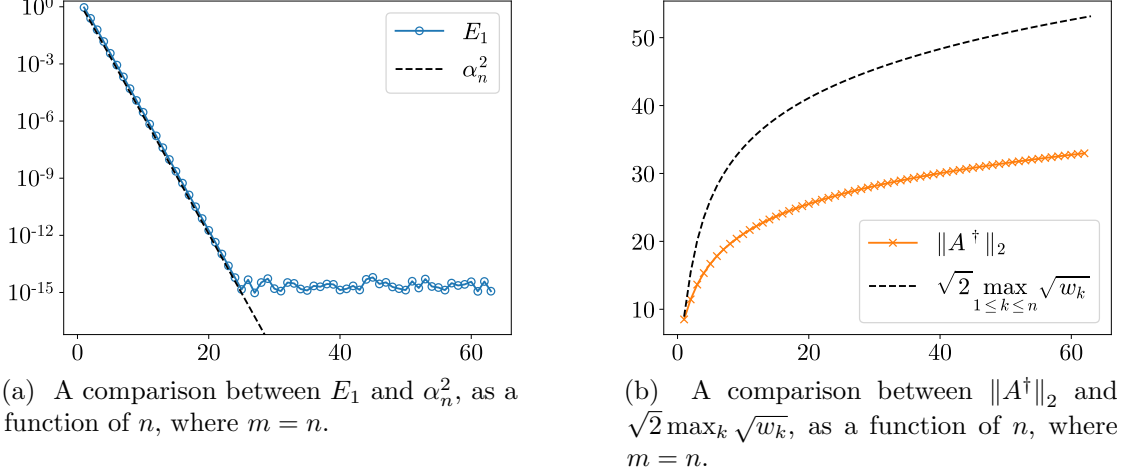


Figure 7: $\gamma = 250$

for all $i = 0, 1, \dots, m-1$. Then, Equation (7) and Equation (105) imply that

$$\begin{aligned}
& \left| \int_0^\infty \int_0^1 e^{-x(+\frac{1}{\gamma-1})} \eta(t) dt dx - \sum_{k=1}^m w_k \int_0^1 e^{-x_k(t+\frac{1}{\gamma-1})} \eta(t) dt \right| \\
&= \left| \int_0^\infty \sum_{i=0}^\infty \alpha_i \left(\int_0^1 u_i(t) \eta(t) dt \right) v_i(x) dx - \sum_{k=1}^m w_k \sum_{i=0}^\infty \alpha_i \left(\int_0^1 u_i(t) \eta(t) dt \right) v_i(x_k) \right| \\
&= \left| \int_0^\infty \sum_{i=m}^\infty \alpha_i \left(\int_0^1 u_i(t) \eta(t) dt \right) v_i(x) dx - \sum_{k=1}^m w_k \sum_{i=m}^\infty \alpha_i \left(\int_0^1 u_i(t) \eta(t) dt \right) v_i(x_k) \right| \\
&\leq \left| \int_0^\infty \sum_{i=m}^\infty \alpha_i \left(\int_0^1 u_i(t) \eta(t) dt \right) v_i(x) dx \right| + \left| \sum_{k=1}^m w_k \sum_{i=m}^\infty \alpha_i \left(\int_0^1 u_i(t) \eta(t) dt \right) v_i(x_k) \right| \\
&\leq \|\eta\|_{L^\infty[0,1]} (A_m^1 + A_m^{\infty,1} \|w\|_1), \tag{106}
\end{aligned}$$

where A_m^1 and $A_m^{\infty,1}$ are defined in Equation (63) and Equation (65), respectively. It follows from Observation 4.1 that

$$E_2 := \max_{0 \leq i, j \leq n-1} \left| \int_0^\infty \alpha_i v_i(x) \cdot \alpha_j v_j(x) dx - \sum_{k=1}^m \frac{w_k}{2} \alpha_i v_i\left(\frac{x_k}{2}\right) \cdot \alpha_j v_j\left(\frac{x_k}{2}\right) \right| \leq A_m^1 + A_m^{\infty,1} \|w\|_1. \tag{107}$$

Since $A_m^1 \approx \alpha_m$, $A_m^{\infty,1} \approx \alpha_m$, and $A_m^{\infty,1} \|w\|_1 \approx \alpha_m \|v_m\|_{L^\infty[0,\infty)} \|w\|_1$, we have $E_2 \lesssim \alpha_m (1 + \|v_m\|_{L^\infty[0,\infty)} \|w\|_1)$, with the size of $\|v_m\|_{L^\infty[0,\infty)} \|w\|_1$ illustrated in Figure 3b. If $E_2 \leq \frac{\alpha_n^2}{2n}$, then Corollary 4.5 guarantees that the norm of $A^\dagger \in \mathbb{R}^{n \times m}$ achieves the bound specified in Equation (96). We see that $E_2 \lesssim \alpha_m (1 + \|v_m\|_{L^\infty[0,\infty)} \|w\|_1) \leq \frac{\alpha_n^2}{2n}$ when $m \approx 2n$. However, instead of choosing m to be so large, we can once again take $m = n$, and use the nodes x_k and the weights w_k rather than $x_k/2$ and $w_k/2$. Unlike the error of the quadrature rule in Equation (102) applied to $\alpha_i u_i \cdot \alpha_j u_j$, for $i, j = 0, 1, \dots, n-1$, which is, in practice, less than α_n^2 , the error of the quadrature rule in Equation (105)

applied to $\alpha_i v_i \cdot \alpha_j v_j$, for $i, j = 0, 1, \dots, n-1$, lies somewhere between α_n^2 and α_n . However, we observe that the special structure of $A \in \mathbb{R}^{n \times n}$ allows the norm of A^\dagger to still attain the bound specified in Equation (96). The results for $\gamma = 10, 50$ and 250 are shown in Figures 5b, 6b and 7b, respectively.

Remark 5.1. It is worth emphasizing that the choice of quadrature nodes is not unique. Any set of quadrature nodes with corresponding weights that satisfy Equation (102) or Equation (105) can be employed for our purposes. In this paper, we choose the roots of u_m and v_m to be the quadrature nodes, since the associated weights are positive and reasonably small, which we have shown in Section 3.

6 Approximation by Singular Powers

In this section, we present a method for approximating a function of the form

$$f(x) = \int_a^b x^\mu \sigma(\mu) d\mu, \quad x \in [0, 1], \quad (108)$$

for some signed Radon measure $\sigma(\mu)$, using a basis of $\{x^{t_j}\}_{j=1}^N$ for some specially chosen points $t_1, t_2, \dots, t_N \in [a, b]$. Our approach involves approximating f by the left singular functions of T_γ , and then discretizing the integral representation of these left singular functions in the form of $\{x^{t_j}\}_{j=1}^N$.

In the following theorem, we establish the existence of such an approximation, and quantify its approximation error.

Theorem 6.1. *Let f be a function of the form Equation (108). Suppose that $\tilde{t}_1, \tilde{t}_2, \dots, \tilde{t}_N$ and $\tilde{w}_1, \tilde{w}_2, \dots, \tilde{w}_N$ are the quadrature nodes and weights of a quadrature rule such that $E_1 \leq \alpha_n^2$, where E_1 is defined in Equation (104). Let $t_j = a + (b-a)\tilde{t}_j$, for all $j = 1, 2, \dots, N$. Then, there exists a vector $c \in \mathbb{R}^N$ such that the function*

$$f_N(x) = \sum_{j=1}^N c_j x^{t_j}, \quad (109)$$

satisfies

$$\|f - f_N\|_{L^\infty[0,1]} \leq |\sigma| \alpha_n \left(\frac{A_n^\infty}{\alpha_n} + U_n V_n + \frac{A_n^\infty}{\alpha_n} U_n^2 \|\tilde{w}\|_1 \right), \quad (110)$$

where A_n^∞ , U_n and V_n are defined in Equation (62), Equation (66) and Equation (67), respectively, and the norm of the coefficient vector c is bounded by

$$\|c\|_2 \leq \|\tilde{w}\|_1 |\sigma| \cdot U_n^2. \quad (111)$$

Proof. Substituting $\omega = -\log x$ into Equation (108), we have

$$\begin{aligned} f(e^{-\omega}) &= \int_a^b e^{-\omega\mu} \sigma(\mu) d\mu, \\ &= \int_0^1 e^{-\tilde{\omega}(\bar{\mu} + \frac{1}{\gamma-1})} (b-a) \sigma((b-a)\bar{\mu} + a) d\bar{\mu}, \quad \tilde{\omega} \in [0, \infty), \end{aligned} \quad (112)$$

where $\bar{\mu} = \frac{\mu-a}{b-a}$, and $\tilde{\omega} = (b-a)\omega$. Since $\{\alpha_i\}_{i=0,1,\dots,\infty}$ decays exponentially, we truncate the SVD of the operator T_γ after n terms and obtain

$$e^{-\omega(t+\frac{1}{\gamma-1})} = \sum_{i=0}^{\infty} v_i(\omega) \alpha_i u_i(t) \approx \sum_{i=0}^{n-1} v_i(\omega) \alpha_i u_i(t). \quad (113)$$

Then, we construct the approximation \tilde{f} to f , defined by

$$\tilde{f}(e^{-\omega}) = \sum_{i=0}^{n-1} \alpha_i \left(\int_0^1 u_i(\bar{\mu})(b-a)\sigma((b-a)\bar{\mu}+a) d\bar{\mu} \right) v_i(\tilde{\omega}). \quad (114)$$

Thus,

$$\begin{aligned} \tilde{f}(x) &= \sum_{i=0}^{n-1} \alpha_i \left(\int_0^1 u_i(\bar{\mu})(b-a)\sigma((b-a)\bar{\mu}+a) d\bar{\mu} \right) v_i(-(b-a)\log x) \\ &= \sum_{i=0}^{n-1} \tilde{c}_i \alpha_i v_i(-(b-a)\log x), \end{aligned} \quad (115)$$

for $x \in [0, 1]$, where

$$\tilde{c}_i = \int_0^1 u_i(\bar{\mu})(b-a)\sigma((b-a)\bar{\mu}+a) d\bar{\mu}. \quad (116)$$

We observe that

$$|\tilde{c}_i| \leq |\sigma| \cdot \|u_i\|_{L^\infty[0,1]}. \quad (117)$$

Thus,

$$\|f - \tilde{f}\|_{L^\infty[0,1]} = \left\| \sum_{i=n}^{\infty} \tilde{c}_i \alpha_i v_i(-(b-a)\log x) \right\|_{L^\infty[0,1]} \leq |\sigma| A_n^\infty, \quad (118)$$

where A_n^∞ is defined in Equation (62) and $A_n^\infty \approx \alpha_n$. According to Equation (8), we have

$$\alpha_i v_i(\omega) = \int_0^1 e^{-\omega(t+\frac{1}{\gamma-1})} u_i(t) dt. \quad (119)$$

Since

$$E_1 = \max_{0 \leq i, j \leq n-1} \left| \int_0^1 \alpha_i u_i(t) \alpha_j u_j(t) dt - \sum_{l=1}^N \tilde{w}_l \alpha_i u_i(\tilde{t}_l) \alpha_j u_j(\tilde{t}_l) \right| \leq \alpha_n^2, \quad (120)$$

for all $i, j = 0, 1, \dots, n-1$, it follows from Corollary 4.3 that

$$\begin{aligned} \tilde{E}_i &:= \left| \int_0^1 e^{-\omega(t+\frac{1}{\gamma-1})} u_i(t) dt - \sum_{l=1}^N \tilde{w}_l e^{-\omega(\tilde{t}_l+\frac{1}{\gamma-1})} u_i(\tilde{t}_l) \right| \\ &\leq \alpha_n V_n + A_n^\infty \|u_i\|_{L^\infty[0,1]} \|\tilde{w}\|_1, \end{aligned} \quad (121)$$

where A_n^∞ and V_n are defined in Equation (62) and Equation (67), respectively.

Recalling Equation (115), we have

$$\tilde{f}(x) = \sum_{i=0}^{n-1} \tilde{c}_i \alpha_i v_i(-(b-a) \log x), \quad (122)$$

so

$$\left| \tilde{f}(e^{-\frac{\tilde{\omega}}{b-a}}) - \sum_{i=0}^{n-1} \tilde{c}_i \sum_{j=1}^N \tilde{w}_j e^{-\tilde{\omega}(\tilde{t}_j + \frac{1}{\gamma-1})} u_i(\tilde{t}_j) \right| \leq \sum_{i=0}^{n-1} |\tilde{c}_i| \tilde{E}_i, \quad (123)$$

which means that

$$\left| \tilde{f}(e^{-\frac{\tilde{\omega}}{b-a}}) - \sum_{i=0}^{n-1} \tilde{c}_i \sum_{j=1}^N \tilde{w}_j e^{-\tilde{\omega} \tilde{t}_j} u_i(\tilde{t}_j - \frac{1}{\gamma-1}) \right| \leq \sum_{i=0}^{n-1} |\tilde{c}_i| \tilde{E}_i, \quad (124)$$

where $\tilde{\omega} = -(b-a) \log x$ and $\tilde{t}_j = \tilde{t}_j + \frac{1}{\gamma-1}$, for all $j = 1, 2, \dots, N$. Substituting $e^{-\frac{\tilde{\omega}}{b-a}} = x$ into Equation (124), we define the approximation f_N to \tilde{f} ,

$$\begin{aligned} f_N(x) &= \sum_{i=0}^{n-1} \tilde{c}_i \sum_{j=1}^N \tilde{w}_j u_i(\tilde{t}_j - \frac{1}{\gamma-1}) x^{(b-a)\tilde{t}_j}, \\ &:= \sum_{j=1}^N c_j x^{(b-a)\tilde{t}_j}, \quad x \in [0, 1], \end{aligned} \quad (125)$$

where $c_j = \tilde{w}_j \sum_{i=0}^{n-1} \tilde{c}_i u_i(\tilde{t}_j - \frac{1}{\gamma-1})$, for $j = 1, 2, \dots, N$. Letting $t_j = (b-a)\tilde{t}_j$, we have $t_j = (b-a)\tilde{t}_j + a$, for $j = 1, 2, \dots, N$. Equation (125) and Equation (117) imply that

$$\begin{aligned} \|c\|_2 &\leq \|\tilde{w}\|_1 \cdot \max_{1 \leq j \leq N} \left| \sum_{i=0}^{n-1} \tilde{c}_i u_i(\tilde{t}_j - \frac{1}{\gamma-1}) \right| \\ &\leq \|\tilde{w}\|_1 \cdot \sum_{i=0}^{n-1} |\tilde{c}_i| \|u_i\|_{L^\infty[0,1]} \\ &\leq \|\tilde{w}\|_1 |\sigma| \cdot \sum_{i=0}^{n-1} \|u_i\|_{L^\infty[0,1]}^2 \\ &\leq \|\tilde{w}\|_1 |\sigma| \cdot U_n^2, \end{aligned} \quad (126)$$

where U_n is defined in Equation (66). The approximation error of f_N to \tilde{f} can be bounded by

$$\begin{aligned} \|\tilde{f} - f_N\|_{L^\infty[0,1]} &\leq \sum_{i=0}^{n-1} |\tilde{c}_i| \tilde{E}_i \\ &\leq \sum_{i=0}^{n-1} |\sigma| \|u_i\|_{L^\infty[0,1]} (\alpha_n V_n + A_n^\infty \|u_i\|_{L^\infty[0,1]} \|\tilde{w}\|_1) \\ &\leq |\sigma| \cdot (\alpha_n U_n V_n + A_n^\infty \sum_{i=0}^{n-1} \|u_i\|_{L^\infty[0,1]}^2 \|\tilde{w}\|_1) \\ &\leq |\sigma| \cdot (\alpha_n U_n V_n + A_n^\infty U_n^2 \|\tilde{w}\|_1). \end{aligned} \quad (127)$$

Thus, we obtain the bound on the approximation error of f_N to f as

$$\begin{aligned} \|f - f_N\|_{L^\infty[0,1]} &\leq \|f - \tilde{f}\|_{L^\infty[0,1]} + \|\tilde{f} - f_N\|_{L^\infty[0,1]} \\ &\leq |\sigma|\alpha_n \left(\frac{A_n^\infty}{\alpha_n} + U_n V_n + \frac{A_n^\infty}{\alpha_n} U_n^2 \|\tilde{w}\|_1 \right), \end{aligned} \quad (128)$$

which is approximately equal to $|\sigma|\alpha_n$, since $A_n^\infty \approx \alpha_n$, and U_n , V_n and $\|\tilde{w}\|_1$ are small. ■

7 Numerical Approximation and Error Analysis

In the previous section, we have shown that, given any function f of the form Equation (108) and any quadrature rule such that $E_1 \leq \alpha_n^2$, where E_1 is defined in Equation (104), there exists a coefficient vector $c \in \mathbb{R}^N$ such that, letting t_1, t_2, \dots, t_N denote the quadrature nodes shifted to the interval $[a, b]$,

$$f_N(x) = \sum_{j=1}^N c_j x^{t_j} \quad (129)$$

is uniformly close to f , to within an error given by Equation (110).

In this section, we show that, by choosing a quadrature rule with quadrature nodes s_1, s_2, \dots, s_N such that $E_2 \leq \frac{\alpha_n^2}{2n}$, where E_2 is defined in Equation (107), and letting

$$x_j = e^{-\frac{s_j}{b-a}}, \quad (130)$$

for $j = 1, 2, \dots, N$, we can construct an approximation

$$\hat{f}_N(x) = \sum_{j=1}^N \hat{c}_j x^{t_j} \quad (131)$$

which is also uniformly close to f , by numerically solving a linear system

$$Vc = F, \quad (132)$$

for the coefficient vector $\hat{c} \in \mathbb{R}^N$, where

$$V = \begin{pmatrix} x_1^{t_1} & x_1^{t_2} & \dots & x_1^{t_N} \\ x_2^{t_1} & x_2^{t_2} & \dots & x_2^{t_N} \\ \vdots & \vdots & \ddots & \vdots \\ x_N^{t_1} & x_N^{t_2} & \dots & x_N^{t_N} \end{pmatrix} \in \mathbb{R}^{N \times N}, \quad (133)$$

and

$$F = (f(x_1), f(x_2), \dots, f(x_N))^T \in \mathbb{R}^N. \quad (134)$$

The uniform approximation error of \hat{f}_N to f over $[0, 1]$ is bounded in Theorem 7.3. Recall that $E_1 \leq \alpha_n^2$ and $E_2 \leq \frac{\alpha_n^2}{2n}$ when $N \approx 2n$ and the quadrature nodes are chosen to be the roots of $u_N(t)$ and $v_N(x)$ (see Section 5).

In the following lemma, we establish upper bounds on the norm and the residual of the perturbed TSVD solution \hat{c} to the linear system in Equation (132), in terms of the norm of the coefficient vector c in Equation (129).

Lemma 7.1. *Let $V \in \mathbb{R}^{N \times N}$, $F \in \mathbb{R}^N$, and $\epsilon > 0$. Suppose that*

$$\widehat{c}_k = (V + \delta V)_k^\dagger (F + \delta F), \quad (135)$$

where $(V + \delta V)_k^\dagger$ is the pseudo-inverse of the k -TSVD of $V + \delta V$, so that

$$\widehat{\alpha}_k \geq \epsilon \geq \widehat{\alpha}_{k+1}, \quad (136)$$

where $\widehat{\alpha}_k$ and $\widehat{\alpha}_{k+1}$ denote the k th and $(k+1)$ th largest singular values of $V + \delta V$, defining $\widehat{\alpha}_{N+1} := 0$, where $\delta V \in \mathbb{R}^{N \times N}$ and $\delta F \in \mathbb{R}^N$, with

$$\|\delta V\|_2 \leq \epsilon_0 \cdot \mu_1 < \frac{\epsilon}{2}, \quad (137)$$

and

$$\|\delta F\|_2 \leq \epsilon_0 \cdot \mu_2, \quad (138)$$

for some $\epsilon_0, \mu_1, \mu_2 > 0$. Suppose further that

$$Vc = F + \Delta F, \quad (139)$$

for some $\Delta F \in \mathbb{R}^N$ and $c \in \mathbb{R}^N$. Then,

$$\|\widehat{c}_k\|_2 \leq \frac{1}{\widehat{\alpha}_k} (2\epsilon + \widehat{\alpha}_k) \|c\|_2 + \frac{1}{\widehat{\alpha}_k} (\|\Delta F\|_2 + \epsilon_0 \cdot \mu_2), \quad (140)$$

and

$$\|V\widehat{c}_k - (F + \Delta F)\|_2 \leq 5\epsilon \|c\|_2 + \frac{3}{2} \|\Delta F\|_2 + \frac{3}{2} \epsilon_0 \cdot \mu_2. \quad (141)$$

Proof. By Equation (135), we have

$$(V + \delta V)_k \widehat{c}_k = F + \delta F = F + \Delta F - \Delta F + \delta F = F + \Delta F + e, \quad (142)$$

where $e := -\Delta F + \delta F$. Thus, Theorem 2.3 implies that

$$\begin{aligned} \|\widehat{c}_k\|_2 &\leq \frac{1}{\widehat{\alpha}_k} (2\epsilon + \widehat{\alpha}_k) \|c\|_2 + \frac{1}{\widehat{\alpha}_k} \|-\Delta F + \delta F\|_2 \\ &\leq \frac{1}{\widehat{\alpha}_k} (2\epsilon + \widehat{\alpha}_k) \|c\|_2 + \frac{1}{\widehat{\alpha}_k} (\|\Delta F\|_2 + \epsilon_0 \cdot \mu_2), \end{aligned} \quad (143)$$

and that

$$\|V\widehat{c}_k - (F + \Delta F)\|_2 \leq 5\epsilon \|c\|_2 + \frac{3}{2} \|\Delta F\|_2 + \frac{3}{2} \epsilon_0 \cdot \mu_2. \quad (144)$$

■

The following observation bounds the backward error, $\|V\widehat{c}_k - F\|_2$, where \widehat{c}_k is the TSVD solution to the perturbed linear system, defined in Equation (135).

Observation 7.1. According to Lemma 7.1, the TSVD solution \hat{c}_k to the perturbed linear system is bounded by the norm of c , as described in Equation (140), where c is the exact solution to the linear system $Vc = F + \Delta F$, and satisfies Equation (111). Thus, the resulting backward error is bounded by

$$\begin{aligned}\|V\hat{c}_k - F\|_2 &= \|V\hat{c}_k - (F + \Delta F) + \Delta F\|_2 \\ &\leq \|V\hat{c}_k - (F + \Delta F)\|_2 + \|\Delta F\|_2 \\ &\leq 5\epsilon\|c\|_2 + \frac{5}{2}\|\Delta F\|_2 + \frac{3}{2}\epsilon_0 \cdot \mu_2.\end{aligned}\tag{145}$$

Although the interpolation matrix V in the basis of $\{x^{t_j}\}_{j=1}^N$ tends to be ill-conditioned, resulting in a loss of stability in the solution to the linear system in Equation (132), we have shown in Lemma 7.1 and Observation 7.1 that, when the TSVD is used to solve the linear system in Equation (132), the backward error, $\|V\hat{c}_k - F\|_2$, which measures the discrepancy between f and \hat{f}_N at the collocation points, is nonetheless small.

The following lemma bounds the L^∞ -norm of a function of the form Equation (108), in terms of its values at the collocation points $\{x_j\}_{j=1}^N$. The constant appearing in this bound serves the same role as the Lebesgue constant for polynomial interpolation.

Lemma 7.2. *Suppose that s_1, s_2, \dots, s_N and w_1, w_2, \dots, w_N are the nodes and weights of a quadrature rule such that $E_2 \leq \frac{\alpha_n^2}{2n}$, where E_2 is defined in Equation (107), and that the collocation points $X := (x_j)_{j=1}^N$ are defined by the formula $x_j = e^{-\frac{s_j}{b-a}}$, for $j = 1, 2, \dots, N$. Let $f(x)$ be a function of the form Equation (108), for some signed Radon measure σ , and let $f(X) \in \mathbb{R}^N$ be the vector of values of $f(x)$ sampled at X . Then,*

$$\|f\|_{L^\infty[0,1]} \leq \sqrt{2} \cdot \max_{1 \leq j \leq N} \sqrt{w_j} \cdot V_n \cdot \|f(X)\|_2 + |\sigma|A_n^\infty \cdot (1 + \sqrt{N} \cdot \sqrt{2} \max_{1 \leq j \leq N} \sqrt{w_j} \cdot V_n),\tag{146}$$

where A_n^∞ and V_n are defined in Equation (62) and Equation (67), respectively.

Proof. Recall from the proof of Theorem 6.1 that $f(x)$ can be approximated by

$$\tilde{f}(x) = \sum_{i=0}^{n-1} \tilde{c}_i \alpha_i v_i(-(b-a) \log x),\tag{147}$$

such that

$$\|f - \tilde{f}\|_{L^\infty[0,1]} \leq |\sigma|A_n^\infty,\tag{148}$$

where A_n^∞ is defined in Equation (62), and \tilde{c}_i , for $i = 0, 1, \dots, n-1$, is given by Equation (116). Let $\tilde{f}(X) = (\tilde{f}(x_1), \tilde{f}(x_2), \dots, \tilde{f}(x_N))^T$. Since Corollary 4.5 implies that $\|A^\dagger\|_2 < \sqrt{2} \max_{1 \leq j \leq N} \sqrt{w_j}$, where the matrix $A^\dagger \in \mathbb{R}^{n \times N}$ is the pseudo-inverse of A , the coefficient vector \tilde{c} in Equation (147) can be found stably by the formula

$$(\tilde{c}_i \alpha_i) = A^\dagger \tilde{f}(X).\tag{149}$$

From Equation (147), we have

$$\begin{aligned}
\|\tilde{f}\|_{L^\infty[0,1]} &= \left\| \sum_{i=0}^{n-1} \tilde{c}_i \alpha_i v_i(-(b-a) \log x) \right\|_{L^\infty[0,1]} \\
&\leq \|(\tilde{c}_i \alpha_i)\|_2 \sqrt{\sum_{i=0}^{n-1} \|v_i\|_{L^\infty[0,\infty)}^2} \\
&\leq \|A^\dagger\|_2 \cdot \|\tilde{f}(X)\|_2 \cdot V_n \\
&\leq \sqrt{2} \cdot \max_{1 \leq j \leq N} \sqrt{w_j} \cdot \|\tilde{f}(X)\|_2 \cdot V_n,
\end{aligned} \tag{150}$$

where V_n is defined in Equation (67). Since

$$|f(x_j) - \tilde{f}(x_j)| \leq \|f - \tilde{f}\|_{L^\infty[0,1]}, \tag{151}$$

for all $j = 1, 2, \dots, N-1$, we have

$$\|\tilde{f}(X)\|_2 \leq \sqrt{N} \|f - \tilde{f}\|_{L^\infty[0,1]} + \|f(X)\|_2. \tag{152}$$

It follows that

$$\begin{aligned}
\|f\|_{L^\infty[0,1]} &\leq \|f - \tilde{f}\|_{L^\infty[0,1]} + \|\tilde{f}\|_{L^\infty[0,1]} \\
&\leq \|f - \tilde{f}\|_{L^\infty[0,1]} + \sqrt{2} \cdot \max_{1 \leq j \leq N} \sqrt{w_j} \cdot \|\tilde{f}(X)\|_2 \cdot V_n \\
&\leq \|f - \tilde{f}\|_{L^\infty[0,1]} + \sqrt{2} \cdot \max_{1 \leq j \leq N} \sqrt{w_j} \cdot (\sqrt{N} \|f - \tilde{f}\|_{L^\infty[0,1]} + \|f(X)\|_2) \cdot V_n \\
&\leq \sqrt{2} \cdot \max_{1 \leq j \leq N} \sqrt{w_j} \cdot V_n \cdot \|f(X)\|_2 + |\sigma| A_n^\infty \cdot (1 + \sqrt{N} \cdot \sqrt{2} \max_{1 \leq j \leq N} \sqrt{w_j} \cdot V_n).
\end{aligned} \tag{153}$$

■

The following theorem provides an upper bound on the global approximation error of \hat{f}_N to f , when the coefficient vector in the approximation is computed by solving $Vc = F$ using the TSVD.

Theorem 7.3. *Let $f(x)$ be a function of the form Equation (108), for some signed Radon measure $\sigma(\mu)$. Suppose that $\tilde{t}_1, \tilde{t}_2, \dots, \tilde{t}_N$ are the nodes of a quadrature rule such that $E_1 \leq \alpha_n^2$, and that s_1, s_2, \dots, s_N are the nodes of a quadrature rule such that $E_2 \leq \frac{\alpha_n^2}{2n}$, where E_1 and E_2 are defined in Equation (104) and Equation (107), respectively. Let $t_j = (b-a)\tilde{t}_j + a$, for $j = 1, 2, \dots, N$, and let x_1, x_2, \dots, x_N be the collocation points defined by the formula $x_j = e^{-\frac{s_j}{b-a}}$. Suppose that $V \in \mathbb{R}^{N \times N}$ is defined in Equation (133) and $F \in \mathbb{R}^N$ is defined in Equation (134), and let $\epsilon > 0$. Suppose further that*

$$\hat{c}_k = (V + \delta V)_k^\dagger (F + \delta F), \tag{154}$$

where $(V + \delta V)_k^\dagger$ is the pseudo-inverse of the k -TSVD of $V + \delta V$, so that

$$\hat{\alpha}_k \geq \epsilon \geq \hat{\alpha}_{k+1}, \tag{155}$$

where $\hat{\alpha}_k$ and $\hat{\alpha}_{k+1}$ denote the k th and $(k+1)$ th largest singular values of $V + \delta V$, defining $\hat{\alpha}_{N+1} := 0$, where $\delta V \in \mathbb{R}^{N \times N}$ and $\delta F \in \mathbb{R}^N$, with

$$\|\delta V\|_2 \leq \epsilon_0 \cdot \mu_1 < \frac{\epsilon}{2}, \quad (156)$$

and

$$\|\delta F\|_2 \leq \epsilon_0 \cdot \mu_2, \quad (157)$$

for some $\epsilon_0, \mu_1, \mu_2 > 0$. Let

$$\hat{f}_N(x) = \sum_{j=1}^N \hat{c}_{k,j} x^{t_j}, \quad (158)$$

with \hat{c}_k defined in Equation (154). Then,

$$\begin{aligned} & \|f - \hat{f}_N\|_{L^\infty[0,1]} \\ & \leq \sqrt{2} \cdot \max_{1 \leq j \leq N} \sqrt{w_j} \cdot V_n \cdot \left(5\epsilon \cdot \|\tilde{w}\|_1 |\sigma| \cdot U_n^2 + \frac{5}{2} \sqrt{N} \cdot |\sigma| \alpha_n \left(\frac{A_n^\infty}{\alpha_n} + U_n V_n + \frac{A_n^\infty}{\alpha_n} U_n^2 \|\tilde{w}\|_1 \right) \right. \\ & \quad \left. + \frac{3}{2} \epsilon_0 \cdot \mu_2 \right) + (|\sigma| + \sqrt{N} \|\hat{c}_k\|_2) \cdot A_n^\infty \cdot (1 + \sqrt{N} \cdot \sqrt{2} \max_{1 \leq j \leq N} \sqrt{w_j} \cdot V_n), \end{aligned} \quad (159)$$

where

$$\begin{aligned} \|\hat{c}_k\|_2 & \leq \frac{1}{\hat{\alpha}_k} (2\epsilon + \hat{\alpha}_k) \|\tilde{w}\|_1 |\sigma| \cdot U_n^2 + \frac{1}{\hat{\alpha}_k} \left(\sqrt{N} \cdot |\sigma| \alpha_n \left(\frac{A_n^\infty}{\alpha_n} + U_n V_n + \frac{A_n^\infty}{\alpha_n} U_n^2 \|\tilde{w}\|_1 \right) \right. \\ & \quad \left. + \epsilon_0 \cdot \mu_2 \right). \end{aligned} \quad (160)$$

Proof. We observe that

$$\hat{f}_N(x) = \int_a^b x^\mu \hat{\sigma}_N(\mu) d\mu, \quad (161)$$

for the signed Radon measure

$$\hat{\sigma}_N(t) = \sum_{j=1}^N \hat{c}_{k,j} \delta(t - t_j), \quad (162)$$

where $\delta(t)$ is the Dirac delta function. Therefore, $f(x) - \hat{f}_N(x)$ can be rewritten as

$$f(x) - \hat{f}_N(x) = \int_a^b x^\mu (\sigma(\mu) - \hat{\sigma}_N(\mu)) d\mu, \quad (163)$$

where $\sigma(\mu)$ is defined in Equation (108). By Theorem 6.1, there exists a vector $c \in \mathbb{R}^N$, such that

$$f_N(x) = \sum_{j=1}^N c_j x^{t_j} \quad (164)$$

is uniformly close to f , with an error bounded by Equation (110). Let $X := (x_j)_{j=1}^N$ and $\Delta F := f(X) - f_N(X)$. Then,

$$\begin{aligned}\|\Delta F\|_2 &\leq \sqrt{N} \cdot \|f - f_N\|_{L^\infty[0,1]} \\ &\leq \sqrt{N} \cdot |\sigma| \alpha_n \left(\frac{A_n^\infty}{\alpha_n} + U_n V_n + \frac{A_n^\infty}{\alpha_n} U_n^2 \|\tilde{w}\|_1 \right),\end{aligned}\quad (165)$$

where A_n^∞ , U_n and V_n are defined in Equation (62), Equation (66) and Equation (67), respectively. By Equation (145) and Equation (111), we have

$$\begin{aligned}\|f(X) - \hat{f}_N(X)\|_2 &= \|V\hat{c}_k - F\|_2 \\ &\leq 5\epsilon \|c\|_2 + \frac{5}{2} \|\Delta F\|_2 + \frac{3}{2} \epsilon_0 \cdot \mu_2 \\ &\leq 5\epsilon \cdot \|\tilde{w}\|_1 |\sigma| \cdot U_n^2 + \frac{5}{2} \sqrt{N} \cdot |\sigma| \alpha_n \left(\frac{A_n^\infty}{\alpha_n} + U_n V_n + \frac{A_n^\infty}{\alpha_n} U_n^2 \|\tilde{w}\|_1 \right) + \frac{3}{2} \epsilon_0 \cdot \mu_2,\end{aligned}\quad (166)$$

where \tilde{w} is the vector of the quadrature weights such that $E_1 \leq \alpha_n^2$. It follows from Lemma 7.2 that the uniform error of the approximation of \hat{f}_N to f is bounded as

$$\begin{aligned}\|f - \hat{f}_N\|_{L^\infty[0,1]} &\leq \sqrt{2} \cdot \max_{1 \leq j \leq N} \sqrt{w_j} \cdot V_n \cdot \left(5\epsilon \cdot \|\tilde{w}\|_1 |\sigma| \cdot U_n^2 + \frac{5}{2} \sqrt{N} \cdot |\sigma| \alpha_n \left(\frac{A_n^\infty}{\alpha_n} + U_n V_n + \frac{A_n^\infty}{\alpha_n} U_n^2 \|\tilde{w}\|_1 \right) \right. \\ &\quad \left. + \frac{3}{2} \epsilon_0 \cdot \mu_2 \right) + |\sigma - \hat{\sigma}_N| A_n^\infty \cdot (1 + \sqrt{N} \cdot \sqrt{2} \max_{1 \leq j \leq N} \sqrt{w_j} \cdot V_n).\end{aligned}\quad (167)$$

Since $|\sigma - \hat{\sigma}_N| \leq |\sigma| + |\hat{\sigma}_N|$ and $|\hat{\sigma}_N| \leq \|\hat{c}_k\|_1$, we have

$$\begin{aligned}\|f - \hat{f}_N\|_{L^\infty[0,1]} &\leq \sqrt{2} \cdot \max_{1 \leq j \leq N} \sqrt{w_j} \cdot V_n \cdot \left(5\epsilon \cdot \|\tilde{w}\|_1 |\sigma| \cdot U_n^2 + \frac{5}{2} \sqrt{N} \cdot |\sigma| \alpha_n \left(\frac{A_n^\infty}{\alpha_n} + U_n V_n + \frac{A_n^\infty}{\alpha_n} U_n^2 \|\tilde{w}\|_1 \right) \right. \\ &\quad \left. + \frac{3}{2} \epsilon_0 \cdot \mu_2 \right) + (|\sigma| + \|\hat{c}_k\|_1) \cdot A_n^\infty \cdot (1 + \sqrt{N} \cdot \sqrt{2} \max_{1 \leq j \leq N} \sqrt{w_j} \cdot V_n) \\ &\leq \sqrt{2} \cdot \max_{1 \leq j \leq N} \sqrt{w_j} \cdot V_n \cdot \left(5\epsilon \cdot \|\tilde{w}\|_1 |\sigma| \cdot U_n^2 + \frac{5}{2} \sqrt{N} \cdot |\sigma| \alpha_n \left(\frac{A_n^\infty}{\alpha_n} + U_n V_n + \frac{A_n^\infty}{\alpha_n} U_n^2 \|\tilde{w}\|_1 \right) \right. \\ &\quad \left. + \frac{3}{2} \epsilon_0 \cdot \mu_2 \right) + (|\sigma| + \sqrt{N} \|\hat{c}_k\|_2) \cdot A_n^\infty \cdot (1 + \sqrt{N} \cdot \sqrt{2} \max_{1 \leq j \leq N} \sqrt{w_j} \cdot V_n),\end{aligned}\quad (168)$$

where $\|\hat{c}_k\|_2$ is bounded by substituting Equation (111) and Equation (165) into Equation (140),

$$\begin{aligned}\|\hat{c}_k\|_2 &\leq \frac{1}{\hat{\alpha}_k} (2\epsilon + \hat{\alpha}_k) \|c\|_2 + \frac{1}{\hat{\alpha}_k} (\|\Delta F\|_2 + \epsilon_0 \cdot \mu_2) \\ &\leq \frac{1}{\hat{\alpha}_k} (2\epsilon + \hat{\alpha}_k) \|\tilde{w}\|_1 |\sigma| \cdot U_n^2 + \frac{1}{\hat{\alpha}_k} \left(\sqrt{N} \cdot |\sigma| \alpha_n \left(\frac{A_n^\infty}{\alpha_n} + U_n V_n + \frac{A_n^\infty}{\alpha_n} U_n^2 \|\tilde{w}\|_1 \right) \right. \\ &\quad \left. + \epsilon_0 \cdot \mu_2 \right).\end{aligned}\quad (169)$$

■

Remark 7.2. By ignoring all the small terms in Equation (168) and Equation (169), and recalling that $A_n^\infty \approx \alpha_n$, we have

$$\|f - \hat{f}_N\|_{L^\infty[0,1]} \lesssim (\epsilon + \alpha_n)|\sigma| + \epsilon_0 \cdot \mu_2 + \alpha_n \|\hat{c}_k\|_2, \quad (170)$$

where

$$\|\hat{c}_k\|_2 \lesssim \left(\frac{\epsilon}{\hat{\alpha}_k} + 1 + \frac{\alpha_n}{\hat{\alpha}_k}\right)|\sigma| + \frac{\epsilon_0}{\hat{\alpha}_k} \mu_2. \quad (171)$$

Thus,

$$\|f - \hat{f}_N\|_{L^\infty[0,1]} \lesssim \left(\epsilon + \alpha_n + \frac{\alpha_n \epsilon}{\hat{\alpha}_k} + \frac{\alpha_n^2}{\hat{\alpha}_k}\right)|\sigma| + \epsilon_0 \cdot \mu_2 + \frac{\alpha_n}{\hat{\alpha}_k} \epsilon_0 \cdot \mu_2. \quad (172)$$

Neglecting all the insignificant terms, the accuracy of the approximation depends on α_n , ϵ , $\hat{\alpha}_k$ and $|\sigma|$, as well as the machine precision ϵ_0 .

Recalling that $\hat{\alpha}_k \geq \epsilon$. If we choose $\epsilon \approx \alpha_n$ in Equation (172), then $\frac{\alpha_n}{\hat{\alpha}_k} \leq \frac{\alpha_n}{\epsilon} \approx 1$ and, accordingly,

$$\begin{aligned} \|f - \hat{f}_N\|_{L^\infty[0,1]} &\lesssim (\epsilon + \alpha_n)|\sigma| + \epsilon_0 \mu_2 \\ &\approx \alpha_n |\sigma| + \epsilon_0 \mu_2. \end{aligned} \quad (173)$$

Thus, the approximation error can achieve a bound that is roughly proportional to $\alpha_n |\sigma|$. Otherwise, if ϵ is significantly smaller than α_n , then the error will exceed $\alpha_n |\sigma|$ because of the term $\frac{\alpha_n^2}{\hat{\alpha}_k}$.

8 Extension from Measures to Distributions

In Section 7, we presented an algorithm for approximating functions of the form

$$f(x) = \int_a^b x^\mu \sigma(\mu) d\mu, \quad x \in [0, 1], \quad (174)$$

where σ is a signed Radon measure, and derived an estimate for the uniform error of the approximation in Theorem 7.3. In this section, we observe that this same algorithm can be applied more generally to functions of the form

$$f(x) = \langle \sigma(\mu), x^\mu \rangle, \quad (175)$$

where $\sigma \in \mathcal{D}'(\mathbb{R})$ is a distribution supported on the interval $[a, b]$. Since every distribution with compact support has a finite order, it follows that $\sigma \in C^m([a, b])^*$ for some order $m \geq 0$.

Recall that

$$|\langle \sigma, \varphi \rangle| \leq \|\sigma\|_{C^m([a,b])^*} \cdot \|\varphi\|_{C^m([a,b])}, \quad (176)$$

where

$$\|\varphi\|_{C^m([a,b])} = \sum_{n=0}^m \sup_{x \in [a,b]} |\varphi^{(n)}|, \quad (177)$$

and

$$\|\sigma\|_{C^m([a,b])^*} = \sup_{\substack{\varphi \in C^m([a,b]) \\ \|\varphi\|_{C^m([a,b])}=1}} |\sigma(\varphi)|. \quad (178)$$

We can use the algorithm of Section 7 to approximate a function of the form Equation (175), where the approximation error is bounded by the following theorem, which generalizes Theorem 7.3.

Theorem 8.1. *Let $f(x)$ be a function of the form Equation (175), Suppose that $\tilde{t}_1, \tilde{t}_2, \dots, \tilde{t}_N$ are the nodes of a quadrature rule such that $E_1 \leq \alpha_n^2$, and that s_1, s_2, \dots, s_N are the nodes of a quadrature rule such that $E_2 \leq \frac{\alpha_n^2}{2n}$, where E_1 and E_2 are defined in Equation (104) and Equation (107), respectively. Let $t_j = (b-a)t_j + a$, for $j = 1, 2, \dots, N$, and let x_1, x_2, \dots, x_N be the collocation points defined by the formula $x_j = e^{-\frac{s_j}{b-a}}$. Suppose that $V \in \mathbb{R}^{N \times N}$ is defined in Equation (133) and $F \in \mathbb{R}^N$ is defined in Equation (134), and let $\epsilon > 0$. Suppose further that*

$$\hat{c}_k = (V + \delta V)_k^\dagger (F + \delta F), \quad (179)$$

where $(V + \delta V)_k^\dagger$ is the pseudo-inverse of the k -TSVD of $V + \delta V$, so that

$$\hat{\alpha}_k \geq \epsilon \geq \hat{\alpha}_{k+1}, \quad (180)$$

where $\hat{\alpha}_k$ and $\hat{\alpha}_{k+1}$ denote the k th and $(k+1)$ th largest singular values of $V + \delta V$, defining $\hat{\alpha}_{N+1} := 0$, where $\delta V \in \mathbb{R}^{N \times N}$ and $\delta F \in \mathbb{R}^N$, with

$$\|\delta V\|_2 \leq \epsilon_0 \cdot \mu_1 < \frac{\epsilon}{2}, \quad (181)$$

and

$$\|\delta F\|_2 \leq \epsilon_0 \cdot \mu_2, \quad (182)$$

for some $\epsilon_0, \mu_1, \mu_2 > 0$. Let

$$\hat{f}_N(x) = \sum_{j=1}^N \hat{c}_{k,j} x^{t_j}, \quad (183)$$

with \hat{c}_k defined in Equation (179). Then,

$$\begin{aligned} & \|f - \hat{f}_N\|_{L^\infty[0,1]} \\ & \leq \sqrt{2} \cdot \max_{1 \leq j \leq N} \sqrt{w_j} \cdot V_n \cdot \left(5\epsilon \cdot \|\tilde{w}\|_1 \cdot \|\sigma\|_{C^m([a,b])^*} \cdot \max_{0 \leq i \leq n-1} \|u_i(\frac{t-a}{b-a})\|_{C^m([a,b])} \cdot U_n^2 \right. \\ & \quad + \frac{5}{2} \sqrt{N} \cdot \|\sigma\|_{C^m([a,b])^*} \cdot \max_{0 \leq i \leq n-1} \|u_i(\frac{t-a}{b-a})\|_{C^m([a,b])} \cdot \alpha_n \left(\frac{A_n^\infty}{\alpha_n} + U_n V_n + \frac{A_n^\infty}{\alpha_n} U_n^2 \|\tilde{w}\|_1 \right) \\ & \quad + \frac{3}{2} \epsilon_0 \cdot \mu_2 \Big) + (\|\sigma\|_{C^m([a,b])^*} \cdot \max_{0 \leq i \leq n-1} \|u_i(\frac{t-a}{b-a})\|_{C^m([a,b])} + \sqrt{N} \|\hat{c}_k\|_2) \cdot A_n^\infty \\ & \quad \cdot (1 + \sqrt{N} \cdot \sqrt{2} \max_{1 \leq j \leq N} \sqrt{w_j} \cdot V_n), \end{aligned} \quad (184)$$

where

$$\begin{aligned} \|\widehat{c}_k\|_2 &\leq \frac{1}{\widehat{\alpha}_k} (2\epsilon + \widehat{\alpha}_k) \|\widetilde{w}\|_1 \cdot \|\sigma\|_{C^m([a,b])^*} \cdot \max_{0 \leq i \leq n-1} \|u_i(\frac{t-a}{b-a})\|_{C^m([a,b])} \cdot U_n^2 \\ &\quad + \frac{1}{\widehat{\alpha}_k} \left(\sqrt{N} \cdot \|\sigma\|_{C^m([a,b])^*} \cdot \max_{0 \leq i \leq n-1} \|u_i(\frac{t-a}{b-a})\|_{C^m([a,b])} \right. \\ &\quad \left. \cdot \alpha_n \left(\frac{A_n^\infty}{\alpha_n} + U_n V_n + \frac{A_n^\infty}{\alpha_n} U_n^2 \|\widetilde{w}\|_1 \right) + \epsilon_0 \cdot \mu_2 \right). \end{aligned} \quad (185)$$

Proof. Since the proof closely resembles the one of Theorem 7.3, we omit it here. The only difference is that $|\sigma|$ in Equation (159) is replaced by $\|\sigma\|_{C^m([a,b])^*} \cdot \max_{0 \leq i \leq n-1} \|u_i(\frac{t-a}{b-a})\|_{C^m([a,b])}$, due to the fact that

$$|\langle \sigma, u_i(\frac{t-a}{b-a}) \rangle| \leq \|\sigma\|_{C^m([a,b])^*} \cdot \|u_i(\frac{t-a}{b-a})\|_{C^m([a,b])}, \quad (186)$$

where the term $\|u_i(\frac{t-a}{b-a})\|_{C^m([a,b])}$ is not negligible, for $m \geq 1$. ■

Note that, when σ is a signed Radon measure, the corresponding distribution has order zero, and $\|\sigma\|_{C([a,b])^*} = |\sigma|$. Thus, in this case, the above bound on $\|f - \widehat{f}_N\|_{L^\infty[0,1]}$ is exactly the same as the bound described in Equation (159).

Remark 8.1. Similar to Remark 7.2, the approximation error is approximately bounded as

$$\begin{aligned} \|f - \widehat{f}_N\|_{L^\infty[0,1]} &\lesssim (\epsilon + \alpha_n + \frac{\alpha_n \epsilon}{\widehat{\alpha}_k} + \frac{\alpha_n^2}{\widehat{\alpha}_k}) \|\sigma\|_{C^m([a,b])^*} \cdot \max_{0 \leq i \leq n-1} \|u_i(\frac{t-a}{b-a})\|_{C^m([a,b])} \\ &\quad + \epsilon_0 \cdot \mu_2 + \frac{\alpha_n}{\widehat{\alpha}_k} \epsilon_0 \cdot \mu_2. \end{aligned} \quad (187)$$

If we choose $\epsilon \approx \alpha_n$, Equation (187) becomes

$$\|f - \widehat{f}_N\|_{L^\infty[0,1]} \lesssim (\epsilon + \alpha_n) \|\sigma\|_{C^m([a,b])^*} \cdot \max_{0 \leq i \leq n-1} \|u_i(\frac{t-a}{b-a})\|_{C^m([a,b])} + \epsilon_0 \cdot \mu_2. \quad (188)$$

9 Numerical Algorithm

The steps of the numerical algorithm for constructing the approximations described in Theorem 7.3 and Theorem 8.1 can be summarized as follows:

1. Given $f(x)$ of the form Equation (108) or Equation (175), compute $\gamma = \frac{b}{a}$.
2. Compute the right singular functions of T_γ , u_0, u_1, \dots , using the algorithm described in Section 4.1 of [17].
3. Compute the left singular functions of T_γ , v_0, v_1, \dots , using the algorithm described in Section 4.1 of [18].
4. Compute the singular values of T_γ , $\alpha_0, \alpha_1, \dots$, using the algorithm described in Section 4.2 of [18].
5. Find n such that $\alpha_n |\sigma|$ is the desired approximation error, where σ is defined in Equation (108) or Equation (175).

6. Set $N = 2n$.
7. Use the algorithm for comrade matrices, described in [31], to compute the roots of $u_N(t)$ as $\tilde{t}_1, \tilde{t}_2, \dots, \tilde{t}_N$, and the roots of $v_N(x)$ as s_1, s_2, \dots, s_N .
8. Rescale s_j by $\frac{s_j}{2}$, for $j = 1, 2, \dots, N$.
9. Obtain the non-integer powers $t_j = (b - a)\tilde{t}_j + a$, and the collocation points $x_j = e^{-\frac{s_j}{b-a}}$, for $j = 1, 2, \dots, N$.
10. Use the non-integer powers and the collocation points to construct $V \in \mathbb{R}^{N \times N}$ as defined in Equation (133) and $F \in \mathbb{R}^N$ as defined in Equation (134).
11. Solve the linear system $Vc = F$ for the coefficient vector \hat{c} , using a TSVD solver with truncation point $\epsilon = \alpha_n$.
12. Construct the approximation $\hat{f}_N(x) = \sum_{j=1}^N \hat{c}_j x^{t_j}$.

In the previous section, we prove that, given any two N -point quadrature rules for which $E_1 \leq \alpha_n^2$ and $E_2 \leq \frac{\alpha_n^2}{2n}$, where E_1 and E_2 are defined in Equation (104) and Equation (107), respectively, one can numerically approximate f by \hat{f}_N uniformly to precision $\alpha_n|\sigma|$. We can construct such quadrature rules by selecting the roots of $u_N(t)$ and $v_N(x)$ for $N \approx 2n$, as shown in Section 5. However, experiments in Section 5 show that, by taking $N = n$ and using the nodes x_k instead of $x_k/2$, we can obtain the same result in practice. Since the function $f(t) = e^{-x(t+\frac{1}{\gamma-1})}u_i(t)$ can be integrated to precision α_n^2 using only $N = n$ points, and the interpolation matrix $A \in \mathbb{R}^{N \times n}$ defined in Equation (91) is well conditioned also for $N = n$, we can achieve the same uniform approximation error of \hat{f}_N to f as described in Equation (159) in Theorem 7.3, for $N = n$.

Previously, we assumed $\epsilon \approx \alpha_n$. When $N = n$, we instead choose ϵ as follows. First, we observe $\|V^{-1}\|_2 \leq \frac{1}{\alpha_n}$, as shown in Figure 8. Letting $\tilde{\alpha}_n$ denote the n -th singular value of V and assuming that δV satisfies $\|\delta V\|_2 \leq \frac{\tilde{\alpha}_n}{2}$, we have

$$\|(V + \delta V)^{-1}\|_2 \leq \frac{1}{\tilde{\alpha}_n - \|\delta V\|_2} \leq \frac{2}{\tilde{\alpha}_n} = 2\|V^{-1}\|_2. \quad (189)$$

Thus, $\|(V + \delta V)^{-1}\|_2 \lesssim \frac{1}{\alpha_n}$, which is equivalent to $\frac{1}{\tilde{\alpha}_n} \lesssim \frac{1}{\alpha_n}$. We have then that $\frac{\alpha_n}{\tilde{\alpha}_n} \lesssim 1$, and therefore, as long as ϵ is not larger than α_n , the resulting approximation error is bounded by

$$\begin{aligned} \|f - \hat{f}_N\|_{L^\infty[0,1]} &\lesssim (\epsilon + \alpha_n) \cdot |\sigma| + \epsilon_0 \mu_2 \\ &\lesssim \alpha_n |\sigma| + \epsilon_0 \mu_2. \end{aligned} \quad (190)$$

In practice, we take $\epsilon = \epsilon_0$.

Therefore, we implement a practical version of the numerical algorithm, which closely follows the one outlined at the beginning of this section, with the following adjustments:

- We replace $N = 2n$ with $N = n$ in Step 6.
- When taking $N = n$, we use the roots of $v_N(x)$, s_1, s_2, \dots, s_N , without scaling them by 2. Thus, we delete Step 8.
- We replace $\epsilon = \alpha_n$ with $\epsilon = \epsilon_0$ in Step 11.

The rest of the steps remain the same.

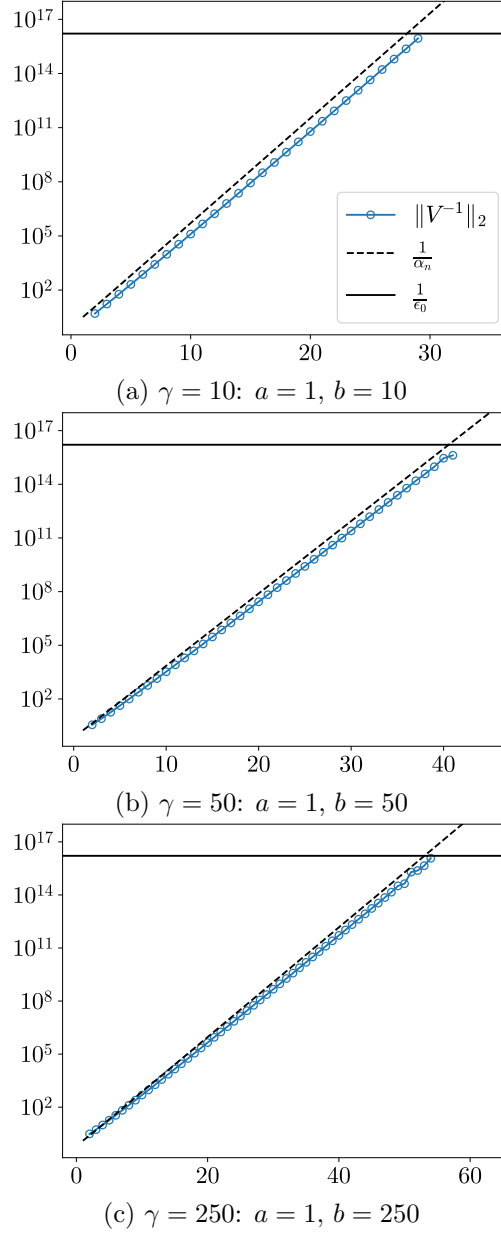


Figure 8: A comparison between $\|V^{-1}\|_2$ and $\frac{1}{\alpha_n}$, as a function of n , for $\gamma = 10, 50, 250$.

10 Numerical Experiments

In this section, we demonstrate the performance of our algorithm with several numerical experiments. Our algorithm was implemented in Fortran 77, and compiled using the GFortran Compiler, version 12.2.0, with -O3 flag. All experiments were conducted on a laptop with 32 GB of RAM and an Intel 12nd Gen Core i7-1270P CPU. A demo of our approximation scheme is provided in <https://doi.org/10.5281/zenodo.8323315>.

All the experiments presented in this section are conducted using the practical version of the numerical algorithm described in Section 9.

10.1 Approximation Over Varying Values of n

In this subsection, we approximate functions of the form $f(x) = \int_a^b x^\mu \sigma(\mu) d\mu$, $x \in [0, 1]$, for the following cases of $\sigma(\mu)$:

$$\sigma_1(\mu) = \frac{1}{\mu}, \quad (191)$$

$$\sigma_2(\mu) = \sin(12\mu), \quad (192)$$

$$\sigma_3(\mu) = e^{-10\mu}, \quad (193)$$

$$\sigma_4(\mu) = \mu \sin(\mu). \quad (194)$$

We estimate $\|f - \hat{f}_N\|_{L^\infty[0,1]}$ by evaluating f and \hat{f}_N at 2000 uniformly distributed points over $[0, 1]$, and finding the maximum error between f and \hat{f}_N at those points. We repeat the experiments for $\gamma = 10, 50, 250$, and plot $\|f - \hat{f}_N\|_{L^\infty[0,1]}/|\sigma|$. The results are displayed in Figures 9 to 11.

It is evident that $\|f - \hat{f}_N\|_{L^\infty[0,1]}/|\sigma|$ remains bounded by α_n , as shown in Section 9, until it reaches a stabilized level that is close to machine precision multiplied by some small constant. Since $\{\alpha_i\}_{i=0,1,\dots,\infty}$ decays exponentially, the approximation exhibits an exponential rate of convergence in N .

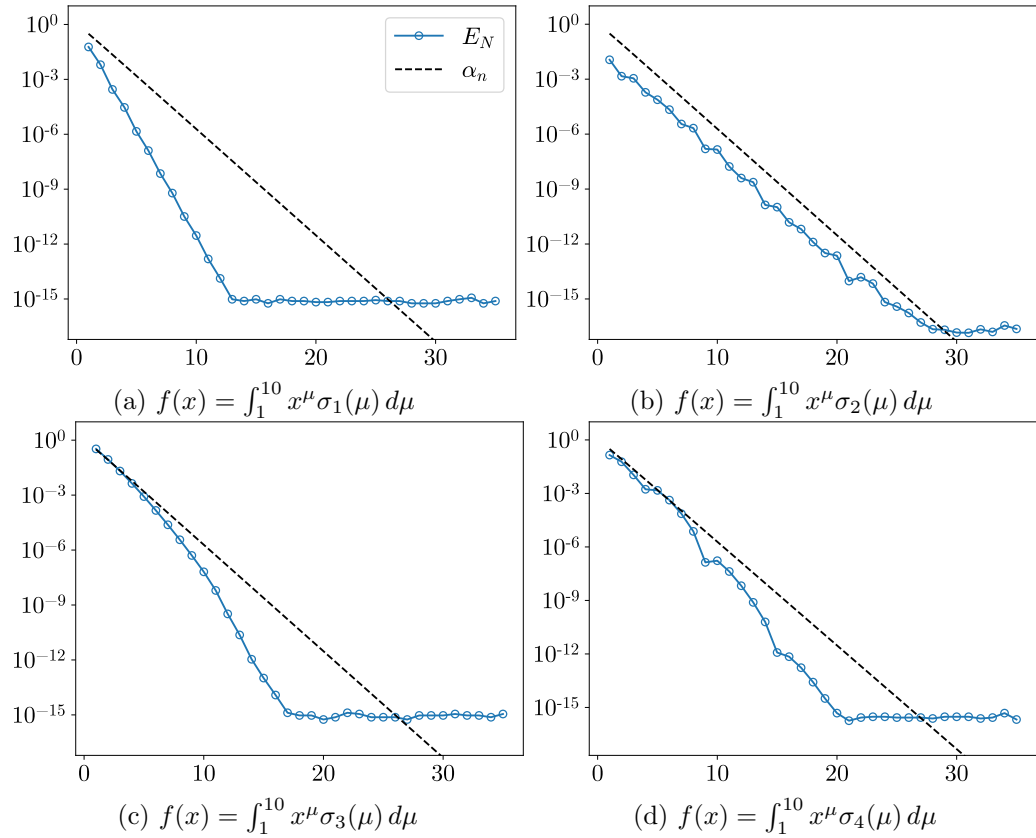


Figure 9: The L^∞ approximation error over $[0, 1]$, $E_N := \frac{\|f - \hat{f}_N\|_{L^\infty[0,1]}}{|\sigma|}$, as a function of n , for $\gamma = 10$.

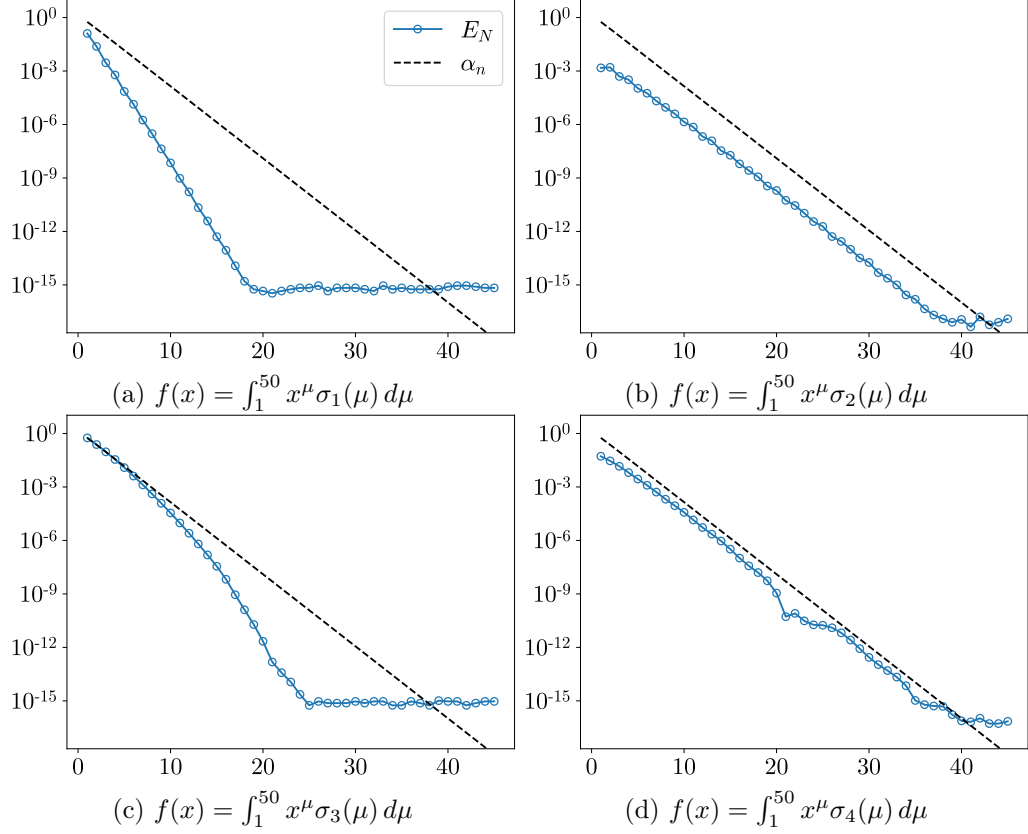


Figure 10: The L^∞ approximation error over $[0, 1]$, $E_N := \frac{\|f - \hat{f}_N\|_{L^\infty[0,1]}}{|\sigma|}$, as a function of n , for $\gamma = 50$.

10.2 Approximation of Non-integer Powers

In this subsection, our goal is to approximate functions of the form $f(x) = \int_a^b x^\mu \sigma(\mu) d\mu$, $x \in [0, 1]$, with

$$\sigma_5(\mu) = \delta(\mu - c), \quad (195)$$

where $c \in [a, b]$. The resulting function is $f(x) = x^c$.

We fix $N = n$, where $\alpha_n \approx \epsilon_0$, and approximate such functions for 1000 values of c distributed logarithmically in the interval $[\frac{a}{1.5}, 1.5b]$. We evaluate f and \hat{f}_N at 1000 uniformly distributed points over $[0, 1]$ to estimate $\|f - \hat{f}_N\|_{L^\infty[0,1]}/|\sigma|$. The results for $\gamma = 10, 50, 250$ are displayed in Figure 12. It can be observed that the approximation error remains accurate up to machine precision multiplied by some small constants, for values of c within the interval $[a, b]$, and grows significantly, for values of c outside $[a, b]$.

We further investigate the approximation error over varying values of n , for $c = a, \frac{a+b}{2}, b$ and $\gamma = 10, 50, 250$, as shown in Figure 13. The approximation error is bounded by α_n multiplied by some small constants, until it stabilizes at a level around machine precision.

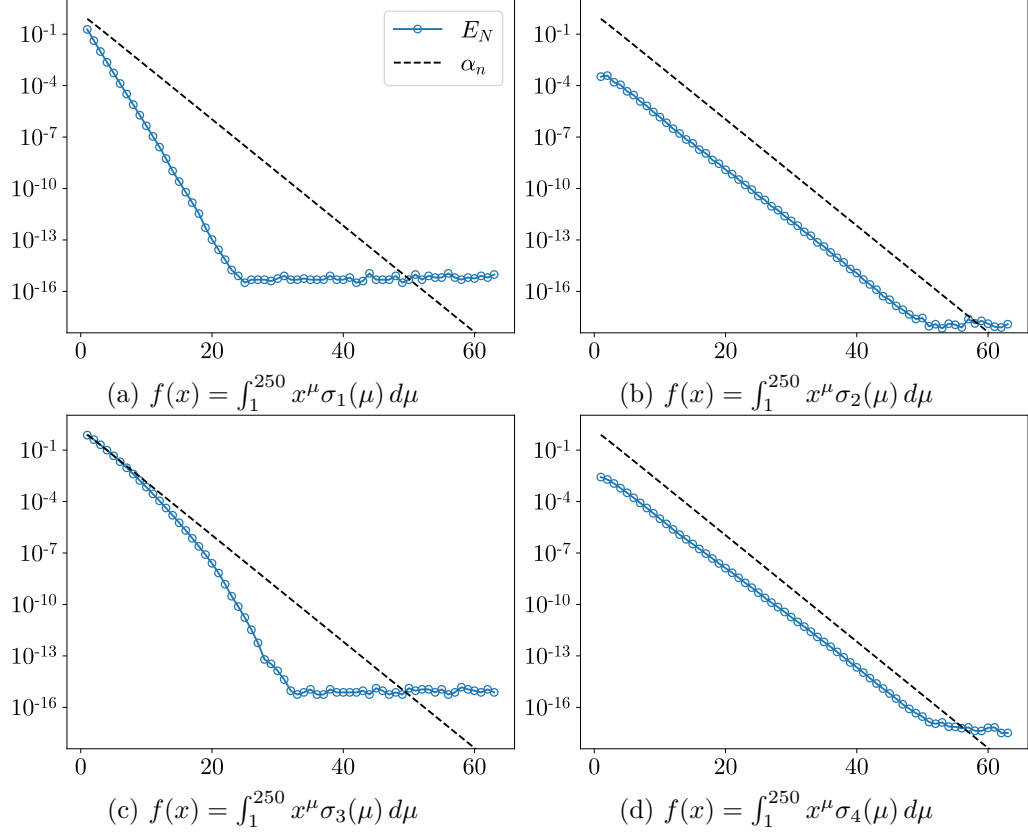


Figure 11: The L^∞ approximation error over $[0, 1]$, $E_N := \frac{\|f - \hat{f}_N\|_{L^\infty[0,1]}}{|\sigma|}$, as a function of n , for $\gamma = 250$.

10.3 Approximation in the Case of Distributions

In this subsection, we assume $\sigma \in \mathcal{D}'(\mathbb{R})$ has the form

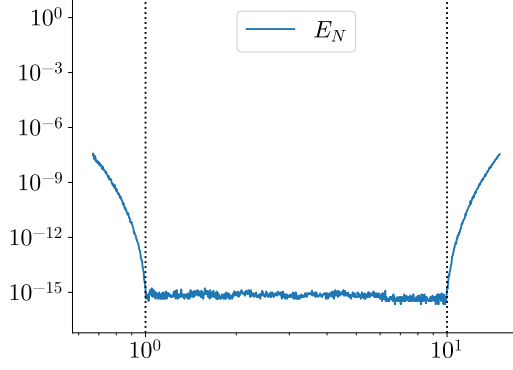
$$\sigma_6(\mu) = (-1)^k \delta^{(k)}(\mu - c), \quad (196)$$

where $k \geq 0$ is an integer, $c \in [a, b]$, and $\delta(t)$ is the Dirac delta function. The resulting function is $f(x) = x^c (\log x)^k$. We evaluate f and \hat{f}_N at 2000 uniformly distributed points in $[0, 1]$ to estimate $\|f - \hat{f}_N\|_{L^\infty[0,1]} / \|\sigma\|_{C^m([a,b])^*}$. The results for $k = 1, 2, \dots, 6$, $c = a$, $\frac{a+b}{2}$, b , and $\gamma = 10, 50, 250$ are shown in Figures 14 to 16.

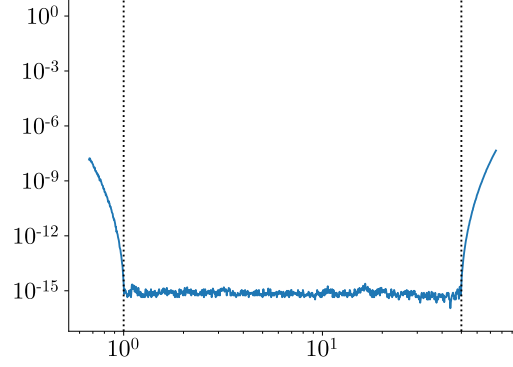
In contrast to the previous cases where σ is a signed Radon measure, the approximation error can increase significantly with k . However, the approximation error is still bounded by $(\epsilon + \alpha_n) \cdot \max_{0 \leq i \leq n-1} \|u_i(\frac{t-a}{b-a})\|_{C^k([a,b])}$, as stated in Theorem 8.1. Furthermore, we observe that the error grows with k , and when $c = a$, the error is closely aligned with the estimated bound, since the function is more singular for smaller c and the approximation error tends to be larger.

10.4 Approximation Over a Simple Arc in the Complex Plane

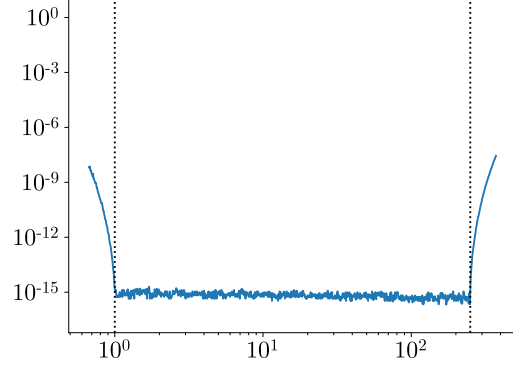
In this subsection, we investigate the performance of our algorithm on simple and smooth arcs in the complex plane. Suppose that $\tilde{\gamma}: [0, 1] \rightarrow \mathbb{C}$, and let $\Gamma = \tilde{\gamma}([0, 1])$. We replace



(a) $n = 28, \gamma = 10: a = 1, b = 10$



(b) $n = 38, \gamma = 50: a = 1, b = 50$



(c) $n = 50, \gamma = 250: a = 1, b = 250$

Figure 12: The L^∞ approximation error of $f(x) = \int_a^b x^\mu \sigma_5(\mu) d\mu = x^c$ over $[0, 1]$, $E_N := \frac{\|f - \hat{f}_N\|_{L^\infty[0,1]}}{|\sigma|}$, as a function of c , for a fixed n such that $\alpha_n \approx \epsilon_0$, and for $\gamma = 10, 50, 250$.

the interpolation matrix V in Equation (133) by a modified interpolation matrix V_Γ , defined by

$$V_\Gamma = \begin{pmatrix} \tilde{\gamma}(x_1)^{t_1} & \tilde{\gamma}(x_1)^{t_2} & \dots & \tilde{\gamma}(x_1)^{t_N} \\ \tilde{\gamma}(x_2)^{t_1} & \tilde{\gamma}(x_2)^{t_2} & \dots & \tilde{\gamma}(x_2)^{t_N} \\ \vdots & \vdots & \ddots & \vdots \\ \tilde{\gamma}(x_N)^{t_1} & \tilde{\gamma}(x_N)^{t_2} & \dots & \tilde{\gamma}(x_N)^{t_N} \end{pmatrix} \in \mathbb{C}^{N \times N}. \quad (197)$$

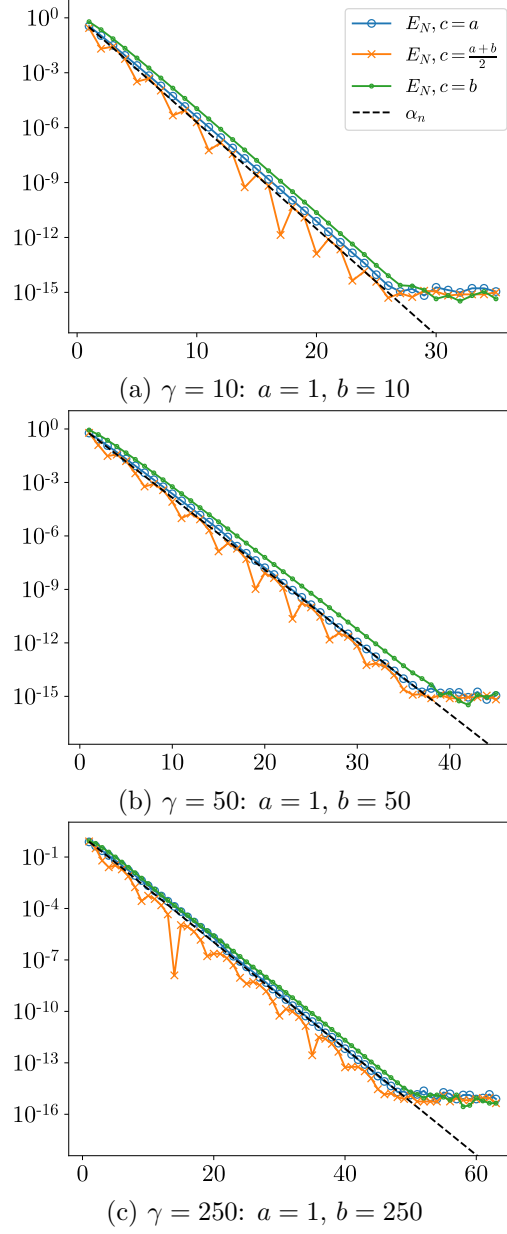


Figure 13: The L^∞ approximation error of $f(x) = \int_a^b x^\mu \sigma_5(\mu) d\mu = x^c$ over $[0, 1]$, $E_N := \frac{\|f - \hat{f}_N\|_{L^\infty[0,1]}}{|\sigma|}$, as a function of n , for $c = a, \frac{a+b}{2}, b$, and $\gamma = 10, 50, 250$.

Specifically, we consider the arcs $\tilde{\gamma}(t) = t + \alpha i(t^2 - t)$, for $\alpha = 0.8, 1.6$ and 2.4 , which are plotted in Figure 17. Our goal is to approximate functions of the form

$$f_\Gamma(t) := \int_a^b \tilde{\gamma}(t)^\mu \sigma(\mu) d\mu, \quad (198)$$

over the arcs $\tilde{\gamma}(t)$, where $t \in [0, 1]$. We apply the algorithm to the functions $f_\Gamma(t)$ where $\sigma(\mu)$ has the forms $\sigma_3(\mu)$ and $\sigma_4(\mu)$, as defined in Equation (193) and Equation (194),

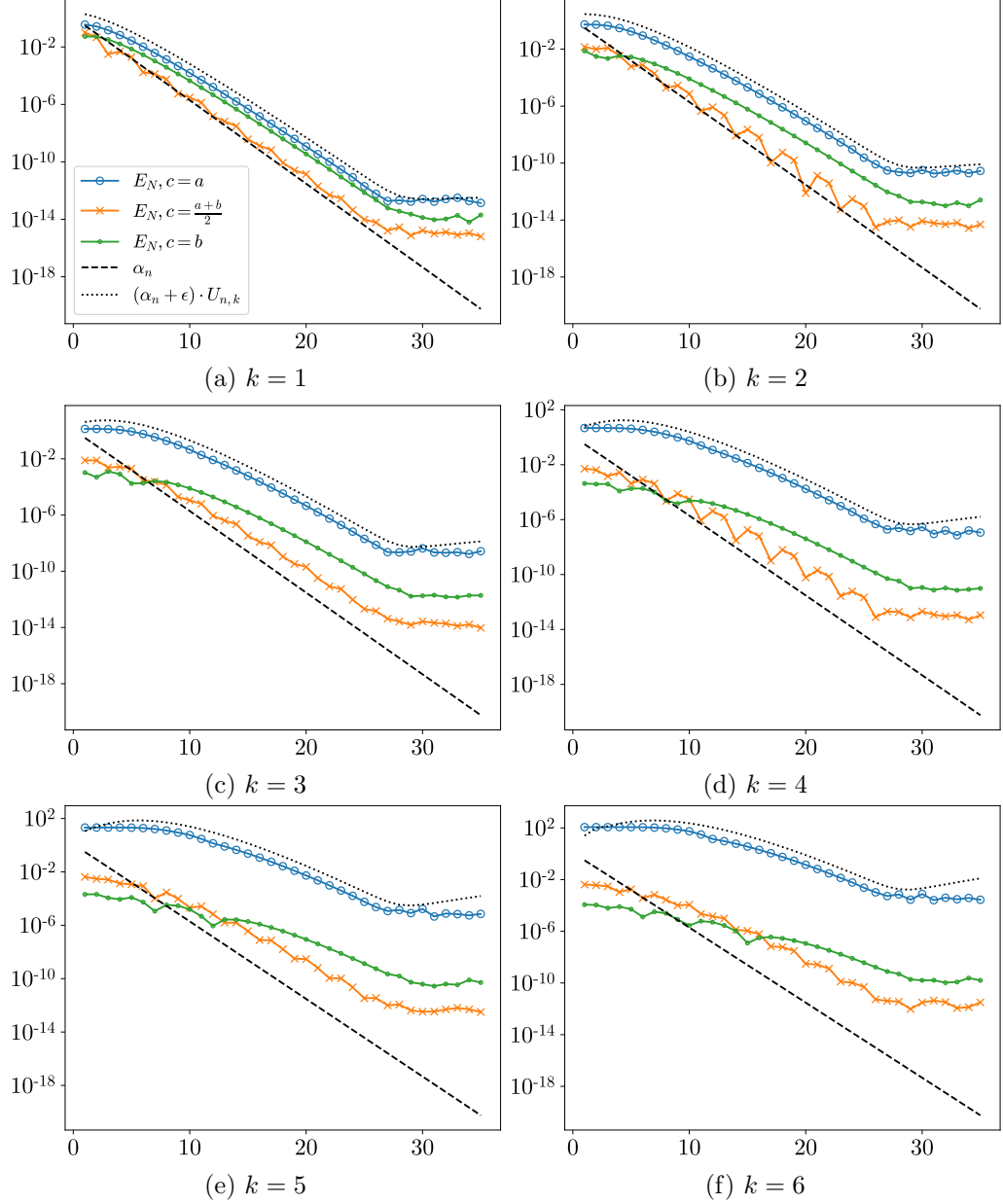


Figure 14: The L^∞ approximation error of $f(x) = \int_1^{10} x^\mu \sigma_6(\mu) d\mu = x^c (\log x)^k$ over $[0, 1]$, $E_N := \frac{\|f - \hat{f}_N\|_{L^\infty[0,1]}}{\|\sigma\|_{C^m([a,b])^*}}$, as a function of n , for $c = a, \frac{a+b}{2}, b, k = 1, \dots, 6$, and $\gamma = 10$. $U_{n,k} := \max_{0 \leq i \leq n-1} \|u_i(\frac{t-a}{b-a})\|_{C^k([a,b])}$.

respectively. The experiments are repeated for $\gamma = 10, 50, 250$, and the results are displayed in Figures 18 to 20.

We also investigate the approximation errors for non-integer powers $f_\Gamma(t) = \tilde{\gamma}(t)^c$ over the arcs $\tilde{\gamma}(t)$, where $c \in [\frac{a}{1.5}, 1.5b]$, following the same procedure as the one described in Section 10.2. The results are displayed in Figure 21.

By analyzing the approximation errors over $\tilde{\gamma}(t)$, for different values of α , we observe

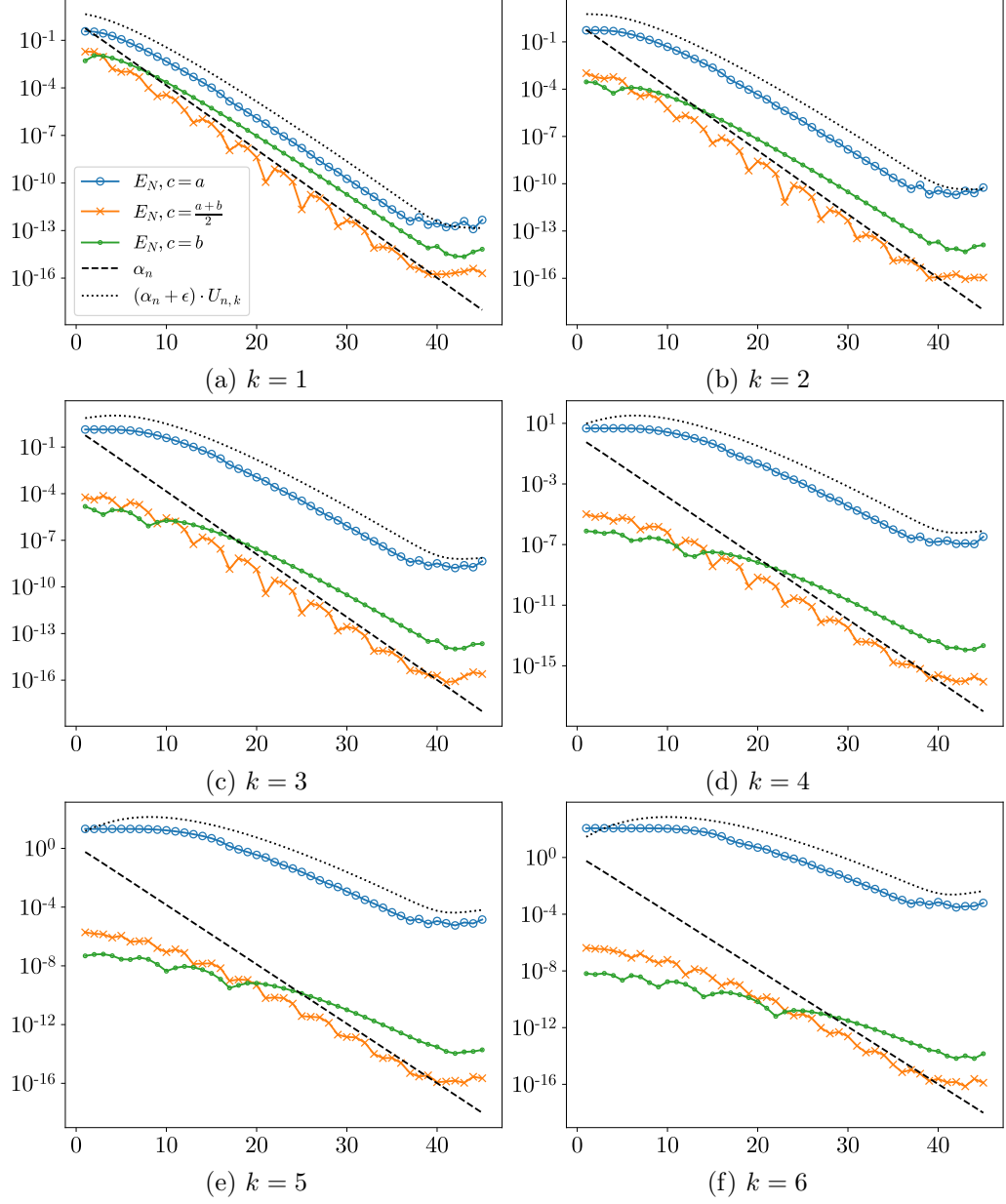


Figure 15: The L^∞ approximation error of $f(x) = \int_1^{50} x^\mu \sigma_6(\mu) d\mu = x^c (\log x)^k$ over $[0, 1]$, $E_N := \frac{\|f - \hat{f}_N\|_{L^\infty[0,1]}}{\|\sigma\|_{C^m([a,b])^*}}$, as a function of n , for $c = a, \frac{a+b}{2}, b$, $k = 1, \dots, 6$, and $\gamma = 50$. $U_{n,k} := \max_{0 \leq i \leq n-1} \left\| u_i \left(\frac{t-a}{b-a} \right) \right\|_{C^k([a,b])}$.

that the approximation error grows with α , and depends on the specific functions being approximated. Generally, when γ is small, the approximation error grows only slightly as the arc becomes more curved, while for large γ , it is possible for the approximation error to grow significantly larger than α_n . When the arc is slightly curved, the approximation performs similarly to the cases where $\tilde{\gamma}(t) = [0, 1]$, with the error bounded by α_n .

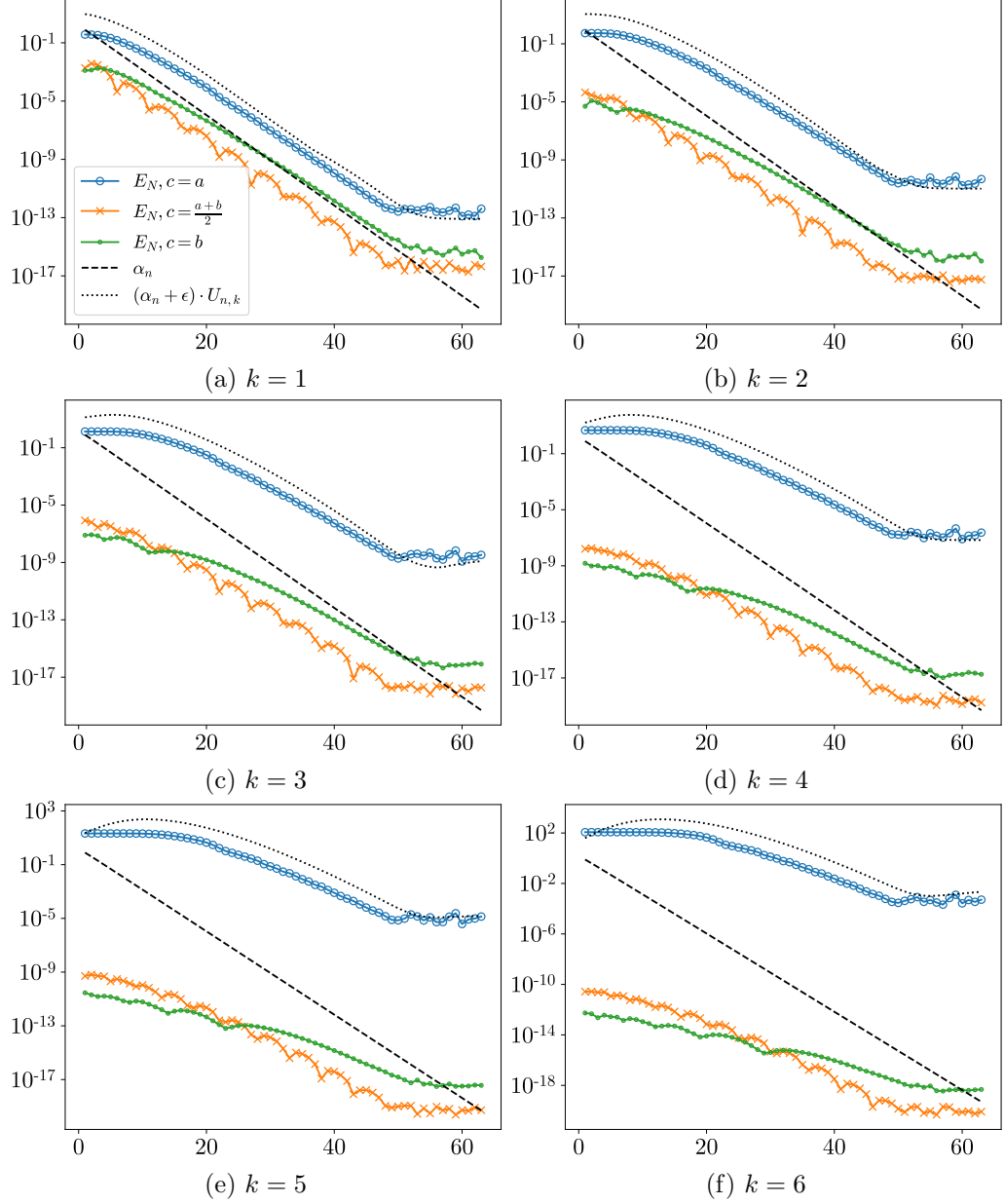


Figure 16: The L^∞ approximation error of $f(x) = \int_1^{250} x^\mu \sigma_6(\mu) d\mu = x^c (\log x)^k$ over $[0, 1]$, $E_N := \frac{\|f - \hat{f}_N\|_{L^\infty[0,1]}}{\|\sigma\|_{C^m([a,b])^*}}$, as a function of n , for $c = a, \frac{a+b}{2}, b, k = 1, \dots, 6$, and $\gamma = 250$. $U_{n,k} := \max_{0 \leq i \leq n-1} \left\| u_i \left(\frac{t-a}{b-a} \right) \right\|_{C^k([a,b])}$.

10.5 Clustering of the Collocation Points

We analyze the clustering behaviour of the collocation points by plotting them for $\gamma = 10, 50, 250$, and for different values of n , as demonstrated in Figures 22 and 23. We observe that the collocation points cluster double-exponentially towards zero, for points that are close to zero, while clustering at a slower rate, rather than double-exponentially, for

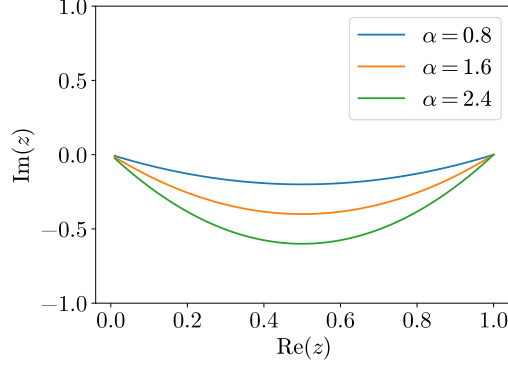


Figure 17: $\tilde{\gamma}(t) = t + \alpha i(t^2 - t)$.

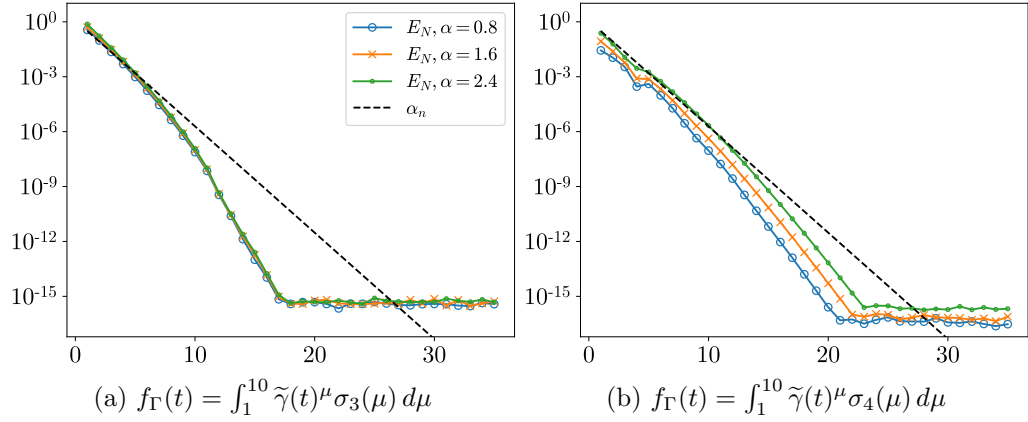


Figure 18: The L^∞ approximation error over $\tilde{\gamma}(t)$, $E_N := \frac{\|f_\Gamma - \hat{f}_N\|_{L^\infty[0,1]}}{|\sigma|}$, as a function of n , for $\alpha = 0.8, 1.6, 2.4$, and $\gamma = 10$.

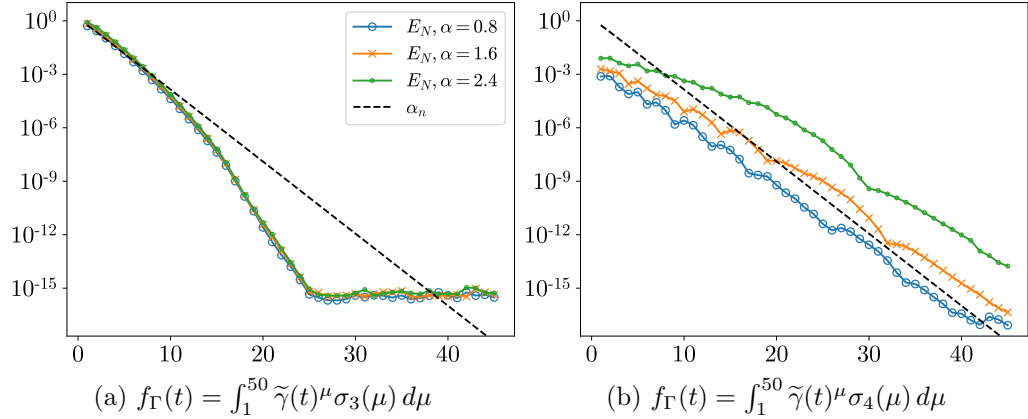


Figure 19: The L^∞ approximation error over $\tilde{\gamma}(t)$, $E_N := \frac{\|f_\Gamma - \hat{f}_N\|_{L^\infty[0,1]}}{|\sigma|}$, as a function of n , for $\alpha = 0.8, 1.6, 2.4$, and $\gamma = 50$.

points that are away from zero. Notably, Figure 22 reveals that the closest collocation point to zero required to achieve an approximation error of size α_n approaches zero at

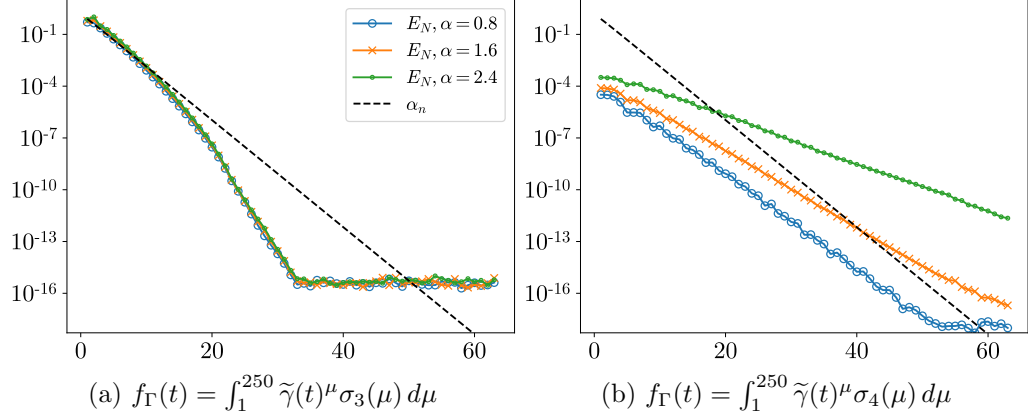
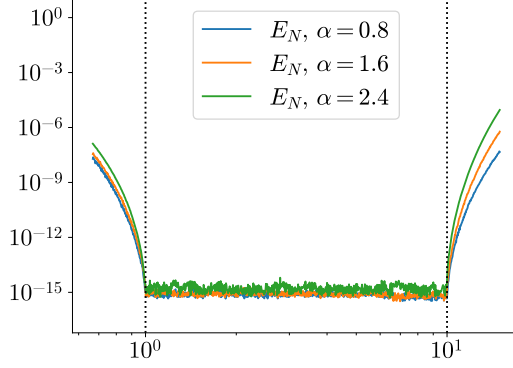


Figure 20: The L^∞ approximation error over $\tilde{\gamma}(t)$, $E_N := \frac{\|f_\Gamma - \hat{f}_N\|_{L^\infty[0,1]}}{|\sigma|}$, as a function of n , for $\alpha = 0.8, 1.6, 2.4$, and $\gamma = 250$.

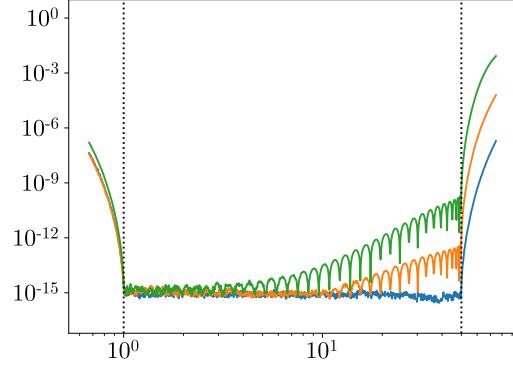
only an exponential rate as n increases. For a fixed approximation error, such as ϵ_0 , the closest collocation point to zero remains at the same distance from zero, for a fixed value of a and varying values of b , as shown in Figure 23.

11 Conclusion

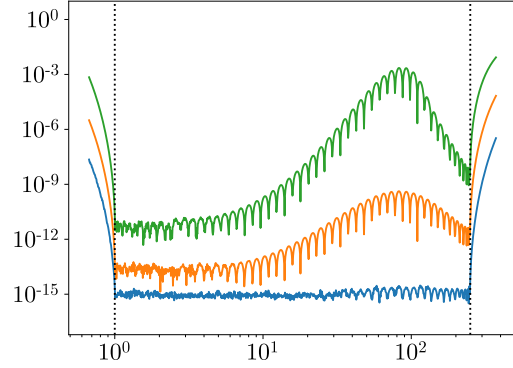
In this paper, we introduce an approach to approximate functions of the form $f(x) = \int_a^b x^\mu \sigma(\mu) d\mu$ over the interval $[0, 1]$, by expansions in a small number of singular powers $x^{t_1}, x^{t_2}, \dots, x^{t_N}$, where $0 < a < b < \infty$ and $\sigma(\mu)$ is some signed Radon measure or some distribution supported on $[a, b]$. Given any desired accuracy ϵ , our method guarantees that the uniform approximation error over the entire interval $[0, 1]$ is bounded by ϵ multiplied by certain small constants. Additionally, the number of basis functions N grows asymptotically as $O(\log \frac{1}{\epsilon})$, and the expansion coefficients can be found by collocating the function at specially chosen collocation points x_1, x_2, \dots, x_N and solving an $N \times N$ linear system numerically. In practice, when $\frac{b}{a} = 10$ and σ is a signed Radon measure, our method requires only approximately $N = 30$ basis functions and collocation points in order to achieve machine precision accuracy. Numerical experiments demonstrate that our method can also be used for approximation over simple smooth arcs in the complex plane. A key feature of our method is that both the basis functions and the collocation points are determined a priori by only the values of a, b , and ϵ . This sets it apart from expert-driven approximation methods, and from other methods that rely on careful selection of parameters to determine the basis functions. For example, the basis functions used in lightning and reciprocal-log approximation are defined by the locations of poles, and the SE-Sinc and DE-Sinc approximations depend on the choices of smooth transformations. Compared to the DE-Sinc approximation, which achieves nearly-exponential rates of convergence at the cost of double-exponentially clustered collocation points, our method uses collocation points that cluster double-exponentially only for points that are close to the singularity, and at a slower rate, rather than double-exponentially, for points that are further away. Moreover, the closest collocation point required to achieve an approximation error of size α_n approaches the singularity at only an



(a) $n = 32, \gamma = 10: a = 1, b = 10$



(b) $n = 42, \gamma = 50: a = 1, b = 50$



(c) $n = 55, \gamma = 250: a = 1, b = 250$

Figure 21: The L^∞ approximation error of $f_\Gamma(t) = \int_a^b \tilde{\gamma}(t)^\mu \sigma_5(\mu) d\mu = \tilde{\gamma}(t)^c$ over $\tilde{\gamma}(t)$, $E_N := \frac{\|f_\Gamma - \hat{f}_N\|_{L^\infty[0,1]}}{|\sigma|}$, as a function of c , for a fixed n such that $\alpha_n \approx \epsilon_0$, $\alpha = 0.8, 1.6, 2.4$, and $\gamma = 10, 50, 250$.

exponential rate as n increases. For a fixed desired accuracy ϵ , the closest collocation point stays at the same distance from the singularity for a fixed value of a and varying values of b . Compared to reciprocal-log approximation, which requires the least-squares solution of an overdetermined linear system with many collocation points, our method involves the solution of a small square linear system to determine the expansion coefficients.

Since our method approximates singular functions accurately by expansions in singular powers, it can be used with existing finite element methods or integral equation methods

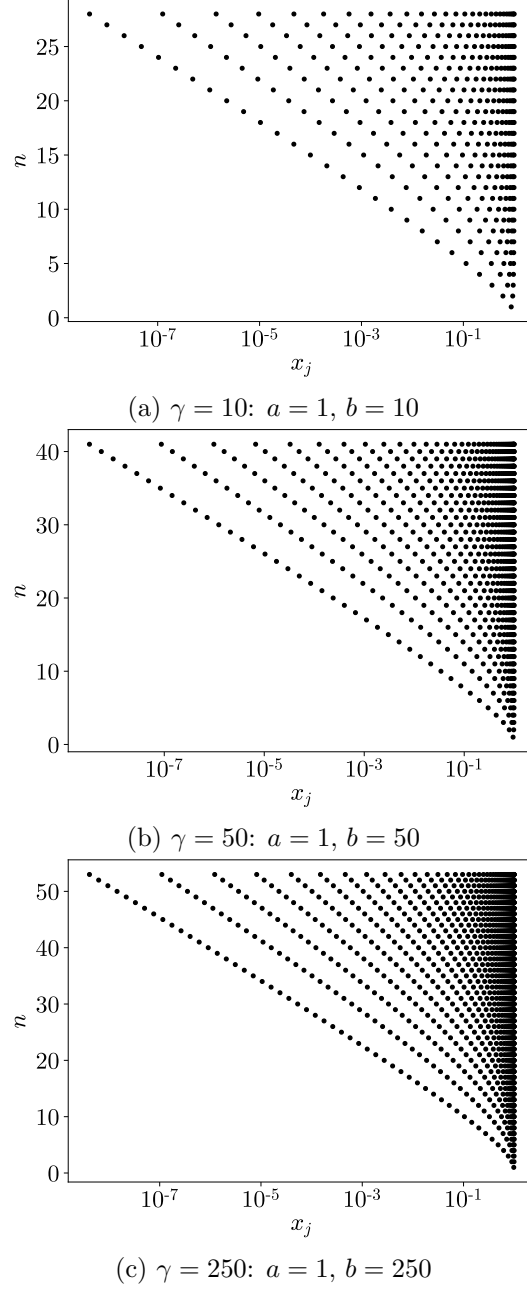


Figure 22: The distribution of collocation points $\{x_j\}_{j=1}^N$ over $[0, 1]$, for values of n such that $\alpha_n \gtrsim \epsilon_0$, and $\gamma = 10, 50, 250$.

to approximate the solutions of PDEs on nonsmooth geometries or with discontinuous data. Typically, the leading singular terms of the asymptotic expansions of solutions near corners are derived from the angles at the corners, and are added to the basis functions of finite element methods to enhance the convergence rates (see, for example, [35], [8], [27]). Now, with only the knowledge that the singular solutions are of the form Equation (108), we can enhance the convergence rates of finite element methods without knowledge of the angles at the corners, by adding all of the singular powers obtained from our method to

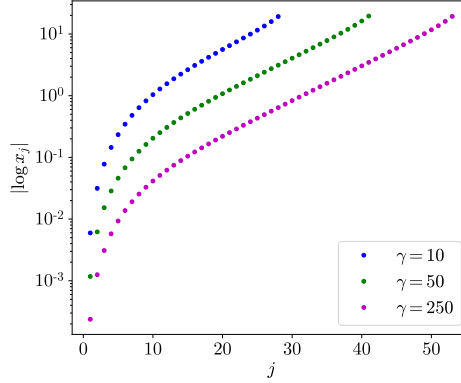


Figure 23: The distribution of collocation points $\{x_j\}_{j=1}^N$ over $[0, 1]$, for fixed values of n such that $\alpha_n \approx \epsilon_0$, and $a = 1$, $b = 10, 50, 250$.

the basis functions. Likewise, the singular powers obtained from our method can be used in integral equation methods for PDEs. In integral equation methods, boundary value problems for PDEs are reformulated as integral equations for boundary charge and dipole densities which represent their solutions. Previously, singular asymptotic expansions of the densities, determined by the angles at the corners, were used to construct special quadrature rules to solve these integral equations (see, for example, [29], [30]). Using only the fact that the singular densities are of the form Equation (108), quadrature rules can instead be developed for only the singular powers obtained from our method, independent of the angles at the corners.

References

- [1] Babuška, I., B. Andersson, B. Guo, J. M. Melenk, and H. S. Oh. “Finite Element Method for Solving Problems with Singular Solutions.” *J. Comput. Appl. Math.* 74 (1996): 51–70.
- [2] Bauer, F.L., and C.T. Fike. “Norms and Exclusion Theorems.” *Numer. Math.* 2.1 (1960): 137–141.
- [3] Bertero, M., P. Boccacci, and E.R. Pike. “On the Recovery and Resolution of Exponential Relaxation Rates from Experimental Data: a Singular-value Analysis of the Laplace Transform Inversion in the Presence of Noise.” *P. Roy. Soc. A-Math. Phy.* 383 (1982): 15–29.
- [4] Beylkin, G., and L. Monzón. “On Approximation of Functions by Exponential Sums.” *Appl. Comput. Harmon. A.* 19.1 (2005): 1063–5203.
- [5] Chen, S., and J. Shen. “Enriched Spectral Methods and Applications to Problems with Weakly Singular Solutions.” *J. Sci. Comput.* 77 (2018): 1468–1489.
- [6] Coppé, V., D. Huybrechs, R. Matthysen, and M. Webb. “The AZ Algorithm for Least Squares Systems with a Known Incomplete Generalized Inverse.” *SIAM J. Matrix Anal. A.* 41.3 (2020): 1237–1259.

- [7] Filip, S., Y. Nakatsukasa, L. N. Trefethen, and B. Beckermann. “Rational Minimax Approximation via Adaptive Barycentric Representations.” *SIAM J. Sci. Comput.* 40.4 (2018): A2427–A2455.
- [8] Fix, G. J., S. Gulati, and G. I. Wakoff. “On the Use of Singular Functions with Finite Element Approximations.” *J. Comput. Phys.* 13.2 (1973): 209–228.
- [9] Fries, T.-P., and T. Belytschko. “The Extended/generalized Finite Element Method: an Overview of the Method and Its Applications.” *Int. J. Numer. Methods Eng.* 84.3 (2010): 253–304.
- [10] Gončar, A. A. “On the Rapidity of Rational Approximation of Continuous Functions with Characteristic Singularities.” *Math. USSR-Sb.* 2.4 (1967): 561–568.
- [11] Gopal, A., and L. N. Trefethen. “New Laplace and Helmholtz Solvers.” *Proc. Natl. Acad. Sci.* 116.21 (2019): 10223–10225.
- [12] Gopal, A., and L. N. Trefethen. “Solving Laplace Problems with Corner Singularities via Rational Functions.” *SIAM J. Numer. Anal.* 57.5 (2019): 2074–2094.
- [13] Gutknecht, M. H., and L. N. Trefethen. “Nonuniqueness of Best Rational Chebyshev Approximations on the Unit Disk.” *J. Approx. Theory* 39.3 (1983): 275–288.
- [14] Hansen, P.C. “The truncated SVD as a Method for Regularization.” *BIT.* 27.4 (1987): 534–553.
- [15] Herremans, A., and D. Huybrechs. “Efficient Function Approximation in Enriched Approximation Spaces.” *IMA J. Numer. Anal.* drae017, 2024.
- [16] Herremans, A., D. Huybrechs, and L.N. Trefethen. “Resolution of Singularities by Rational Functions.” *SIAM J. Numer. Anal.* 61.6 (2023): 2580–2600.
- [17] Lederman, R.R., and V. Rokhlin. “On the Analytical and Numerical Properties of the Truncated Laplace Transform.” *SIAM J. Numer. Anal.* 53.3 (2015): 1214–1235.
- [18] Lederman, R.R., and V. Rokhlin. “On the Analytical and Numerical Properties of the Truncated Laplace Transform. Part II.” *SIAM J. Numer. Anal.* 54.2 (2016): 665–687.
- [19] Lehman, R. S. “Developments at an Analytic Corner of Solutions of Elliptic Partial Differential Equations.” *J. Math. Mech.* 8.5 (1959): 727–760.
- [20] Lucas, T. R., and H. S. Oh. “The Method of Auxiliary Mapping for the Finite Element Solutions of Elliptic Problems Containing Singularities.” *J. Comput. Phys.* 108.2 (1993): 327–342.
- [21] Mori, M. “Discovery of the Double Exponential Transformation and Its Developments.” *Publ. Res. Inst. Math. Sci.* 41 (2005): 897–935.
- [22] Nakatsukasa, Y., and L. N. Trefethen. “An Algorithm for Real and Complex Rational Minimax Approximation.” *SIAM J. Sci. Comput.* 42.5 (2020): A3157–A3179.

- [23] Nakatsukasa, Y., and L. N. Trefethen. “Reciprocal-log Approximation and Planar PDE Solvers.” *SIAM J. Numer. Anal.* 59.6 (2021): 2801–2822.
- [24] Nakatsukasa, Y., O. Sète, and L. N. Trefethen. “The AAA Algorithm for Rational Approximation.” *SIAM J. Sci. Comput.* 40.3 (2018): A1494–A1522.
- [25] Newman, D. J. “Rational Approximation to $|x|$.” *Mich. Math. J.* 11.1 (1964): 11–14.
- [26] Okayama, T., T. Matsuo, and M. Sugihara. “Sinc-collocation Methods for Weakly Singular Fredholm Integral Equations of the Second Kind.” *J. Comput. Appl. Math.* 234.4 (2010): 1211–1227.
- [27] Olson, L. G., G. C. Georgiou, and W. W. Schultz. “An Efficient Finite Element Method for Treating Singularities in Laplace’s Equation.” *J. Comput. Phys.* 96.2 (1991): 391–410.
- [28] Roache, P. J. “A Pseudo-spectral FFT Technique for Non-periodic Problems.” *J. Comput. Phys.* 27.2 (1978): 204–220.
- [29] Serkh, K. “On the Solution of Elliptic Partial Differential Equations on Regions with Corners.” *J. Comput. Phys.* 305 (2016): 150–171.
- [30] Serkh, K., and V. Rokhlin. “On the Solution of the Helmholtz Equation on Regions with Corners.” *Proc. Natl. Acad. Sci.* 113.33 (2016): 9171–9176.
- [31] Serkh, K., and V. Rokhlin. “A Provably Componentwise Backward Stable $O(n^2)$ QR Algorithm for the Diagonalization of Colleague Matrices.” *ArXiv*, 2021.
- [32] Stahl, H. “Best Uniform Rational Approximation of x^α on $[0, 1]$.” *Acta. Math.* 190 (2003): 241–306.
- [33] Stenger, F. “Explicit Nearly Optimal Linear Rational Approximation with Preassigned Poles.” *Math. Comput.* 47.175 (1986): 225–252.
- [34] Stenger, F. “Numerical Methods Based on Sinc and Analytic Functions in numerical Analysis.” *SSCM* Springer-Verlag, 1993.
- [35] Tong, P., and T. H. H. Pian. “On the Convergence of the Finite Element Method for Problems with Singularity.” *Int. J. Solids Struct.* 9.3 (1973): 313–321.
- [36] Trefethen, L. N., Y. Nakatsukasa, and J. A. C. Weideman. “Exponential Node Clustering at Singularities for Rational Approximation, Quadrature, and PDEs.” *Numer. Math.* 147.1 (2021): 227–254.
- [37] Trefethen, L. N. “Approximation Theory and Approximation Practice, Extended Edition.” *Society for Industrial and Applied Mathematics*, 2019.
- [38] Wasow, W. “Asymptotic Development of the Solution of Dirichlet’s Problem at Analytic Corners.” *Duke Math. J.* 24.1 (1957): 47–56.